

# Impact of the slaking method on the mineralogy of natural hydraulic limes and its effects on mortar mechanical properties

Clara Parra-Fernández, Anna Arizzi\*

Departamento de Mineralogía y Petrología, Facultad de Ciencias, Universidad de Granada, Avda. Fuentenueva s/n, 18002 Granada, Spain

## ARTICLE INFO

### Keywords:

Air slaking  
Pre-hydration  
Carbonation  
Hydraulic phases  
Portlandite

## ABSTRACT

The influence of slaking on the properties of natural hydraulic limes (NHL) has been little studied so far. Laboratory-manufactured limes have been produced to investigate the mineralogical changes that occur during the slaking process. Two different hydration methods have been compared: conventional slaking, by adding water in a 1:1 water:CaO ratio, and passive slaking, by exposure of the quicklimes to a relative humidity of  $60 \pm 5\%$  and  $80 \pm 5\%$  RH. The mineralogical evolution of limes was monitored under different slaking conditions using the X-ray diffraction Quantitative Phase Analysis. The resulting NHLs have been used to produce mortars, to assess the influence of the slaking conditions on their mechanical strength. The results show that passive slaking at relative humidities higher than 60% ensures complete transformation of CaO into Ca(OH)<sub>2</sub>, and gives place to natural hydraulic limes with comparable, or even slightly improved properties to those conventionally slaked.

## 1. Introduction

Slaking is one of the steps carried out during the manufacturing of both aerial and hydraulic lime. It consists of the reaction of calcium oxide with water to obtain calcium hydroxide (Eq. (1)):



This reaction involves an increase in temperature (exothermic) as well as in the specific surface area, weight and volume of the lime [1].

It is nowadays widely accepted that the rate of slaking of a quicklime and the maximum temperature reached during this process, which give an indication of its reactivity, are highly dependent on the calcination temperature reached to burn the limestone, together with other factors such as purity and size of the quicklime, burning time and presence of CO<sub>2</sub> in the kiln, as it will be discussed below.

Already one century ago, it was found that T higher than 1100 °C provide a less reactive aerial lime compared to T around 900 °C [2], the latter considered the optimum calcination temperature for aerial lime, as a CaO with higher specific surface area and therefore, reactivity, is obtained [3,4]. For natural hydraulic limes, instead, the optimum burning temperature, which is the one that gives the maximum amount of hydraulic phases and, at the same time, a good reactivity of the quicklime to slaking, is around 1000–1100 °C [5,6].

Regarding the influence of the residence and burning time, different authors has shown that long burning times can affect negatively the reactivity of the quicklime [7–9]. And the burning time is, in turns, dependent on the intrinsic petrographic features (clastic, micritic/sparitic rock textures) and mineralogical composition of the limestones used [9–13]. The presence of impurities is considered another relevant factor for the quicklime reactivity, even more than the specific surface area [14]. On the one hand, it has been found that impurities such as MgO, Fe<sub>2</sub>O<sub>3</sub> and K<sub>2</sub>O may increase sintering phenomena and, therefore, lower calcination temperatures would be recommended for impure limestones to achieve a better reactivity of the quicklime [14]. On the other hand, it has been reported that hydraulic phases, such as larnite, hatrurite, brownmillerite and aluminates phases, may act as sintering inhibitors at  $T > 1250$  °C, and this would explain the lower over-burning tendency of hydraulic limes with respect to pure limes at high temperatures [11].

Not less important, the presence of CO<sub>2</sub> in the kiln has also an influence on the reactivity of CaO towards water. According to Commandré et al. [15], the high CO<sub>2</sub> pressure reached in industrial kilns, which is not desired as it inhibits decarbonation, is overcome by using higher calcination temperatures (1000–1300 °C), which induce sintering of calcium oxide, and therefore lead to a decrease in its specific surface area and to a final lower reactivity of the quicklime towards

\* Corresponding author.

E-mail address: [arizzina@ugr.es](mailto:arizzina@ugr.es) (A. Arizzi).

**Table 1**

Amounts of binder, aggregate and water for mortar elaboration and consistency and bulk density values. CS: conventional slaking; PS60: passive slaking at  $60 \pm 5$  % RH; PS80: passive slaking at  $80 \pm 5$  % RH.

Sample	Condition	Binder (g)	Aggregate (g)	Water (g)	Flow (mm)	Bulk density (kg/m <sup>3</sup> )
M-NHL2	CS	340.77	1022.31	260.39	152.5	2224.47
	PS60	380.39	1141.17	253.2	150	2258.39
	PS80	371.16	1113.48	229.58	152	2253.45
M-NHL3.5	CS	450	1350	275	155.5	2209.18
	PS60	351.43	1054.29	225.72	155.8	2154.28
	PS80	354.6	1063.8	222.3	156	2180.01
M-NHL5	CS	429.83	1289.49	259.92	152	2187.1
	PS60	359.59	1078.65	264.78	155.5	2119.09
	PS80	373.18	1119.54	251.59	155	2055.63

hydration.

Industrially, slaking of quicklime is carried out with a stoichiometric amount of water (1:1 water:CaO ratio), which is added by spraying, or by irrigation, leading to a lime in the form of a powder (also called *dry slaking*) [16]. In the case of aerial lime, slaking can also be carried out under water, namely when an excess of water is used, leading to a lime in the form of a putty or slurry (also called *wet slaking*), whose plasticity and reactivity might be improved by aging under water [17]. The second method was mostly used in the past and in nowadays artisanal processes.

However, to obtain natural hydraulic lime, only dry slaking is carried out. This is because, after the calcination step, the obtained quicklime is generally composed of variable amounts of CaO and different hydraulic phases, and only the former must be hydrated in this phase. The calculation of the correct amount of water to be added to the quicklime is made based on different chemical analytical techniques or methods, which are indicated by both the European (EN 459–2:2021 [18]) and the American (ASTM C25:2017 [19]) standards (e.g. complexometric titration; X-ray fluorescence; Rapid Sugar Test method [20]). However, the amount of CaO in NHLs might be under- or over-estimated, thus leading to a binder with quenched properties. On the one hand, an incomplete slaking would lead to the later hydration of CaO in the mortar producing fissures and fractures due to the volume changes caused by this process. On the other hand, the use of an excess of water might lead to the undesired partial hydration of some hydraulic phases of this binder. Calcium silicates and aluminates are expected to hydrate in the mortar, as they are responsible for the hydraulic hardening and setting of the material, and therefore their premature hydration might lead to a decrease in the final mechanical performance of the mortars [21,22].

Besides the ordinary dry and wet slaking methods described above, also other less common ways of hydrating limes have been reported in literature. For example, *earth-slaking*, where the quicklime is placed in a lime wooden pit and covered with soil for 4–5 years [23], *air-slaking* [24] and *wind-slaking* [25], which both consist in exposing the quicklimes to the moisture of air. According to those studies, these unconventional slaking methods yield limes with greater workability [23] and lower shrinkage [25] than wet-slaked limes, even though these procedures are slower than conventional slaking [25], and may produce more lime lumps in the mortars [23].

To the best of current knowledge, limited research has explored the effects of different methods of slaking on the quality of natural hydraulic lime [24,25], with the majority of studies focusing primarily on aerial lime (lime putty mainly [22,23,26–33]). Studies on natural hydraulic limes are indeed more focused on the influence of water:binder ratio and relative humidity on the outcome of the carbonation and hydration processes of NHL pastes [34–36] and on the properties of the mortars made with them (for example, Lanas et al. [37], Zhang et al. [38], Fusade & Viles [39] and Groot et al. [40]).

Within this context, this study aims to investigate the influence of different slaking methods on the mineralogical composition of NHL limes and on the mechanical properties of their mortars. For this purpose, siliceous limestones with a known chemical-mineralogical

composition and different cementation indexes, suitable for the manufacturing of NHL with different hydraulic degrees, have been calcined under specific calcination conditions, as reported in Parra-Fernández et al. [6], to obtain three types of NHL quicklimes that have been hydrated using three different slaking methods: a conventional slaking, adding a CaO:water ratio of 1:1; and two passive procedures, exposing the quicklimes to constant temperature and different relative humidities (60 and 80 %). The evolution of the slaking process has been monitored by means of quantitative phase analysis (QPA) and, at the end of the process, mortars were prepared and cured for 28 days, in order to assess the influence of the slaking method on their mechanical properties. Previous studies on the laboratory production of hydraulic binders [5,41,42], indeed, support the importance of determining the mechanical properties of the mortars made with them to obtain a complete evaluation of the manufactured binders.

## 2. Materials and methodology

### 2.1. NHL manufacture

The raw materials selected for this study are siliceous limestones and marl-limestones with microcrystalline quartz (*sillex* or flint) from Sierra Elvira (Granada, Andalusia, Spain). More details on sampling and stone characterization can be found in Parra-Fernández et al. [6]. The chemical composition of the raw materials was analysed by X-Ray Fluorescence (FRX) using a S4 PIONEER-BRUKER wavelength dispersive X-ray fluorescence spectrometer, with a Rh tube (60 kV; 150 mA), LIF200/PET/OVO-55 analyser crystals and gas-flow proportional and scintillation detectors. All samples were first ground to powder and then prepared in tablets for the XRF analysis. This technique allowed to obtain the oxides content and to calculate the cementation index (CI, Eq. (2), [43]).

$$CI = \frac{2.8 (\%SiO_2) + 1.1 (\%Al_2O_3) + 0.7 (\%Fe_2O_3)}{(\%CaO) + 1.4 (\%MgO)} \quad (2)$$

As in Parra-Fernández et al. [6], the raw materials used were selected on the basis of their CI values, which are correlated to the hydraulic degree of each NHL [1,5,10,12,43–50], as follows: 0.3–0.5 for NHL2, 0.5–0.7 for NHL3.5, 0.7–1.1 for NHL5. The same calcination conditions as in Parra-Fernández et al. [6] were applied to obtain the NHL quicklimes: 300 g of ground powders ( $\phi < 35 \mu\text{m}$ , according to laser granulometry analysis) in graphite crucibles (109 × 95 × 61 mm); calcination in a Hobersal JM22/16 kiln at 1100 °C (gradient of 7.26 °C/min) and dwell time of 2 h in the kiln.

After calcination, the NHL quicklimes were slaked with three different methods:

1) *Conventional slaking* (CS), by spreading each lime on a  $2 \times 30 \times 40 \text{ cm}^3$  sized tray and spraying water in a 1:1 ratio of calcium oxide:water (CaO amount calculated on the basis of the XRF data). During conventional slaking, the following factors were monitored: 1) duration of the exothermic reaction, due to transformation of CaO into Ca(OH)<sub>2</sub>, and 2) maximum temperature reached. The temperature rise was controlled by

**Table 2** Mineralogical composition, main reactive oxides and CI values of the raw materials and mineralogical composition of calcined products (estimated standard deviations are in brackets). Legend: RM, raw material; C, calcined material.

Sample	Mineralogical composition (wt%)											Chemical composition (%)						
	Calcite	Dolomite	Quartz	Plagioclase	K-feldspar	Illite	Kaolinite	Ilmenite	Amorphous	SiO <sub>2</sub>	Al <sub>2</sub> O <sub>3</sub>	Fe <sub>2</sub> O <sub>3</sub>	MgO	CaO	LOI	CI		
NHL2 RM	80.86 (0.41)	1.99 (0.01)	5.61 (0.03)	0.93 (0.00)	–	2.18 (0.01)	–	0.82 (0.00)	7.61 (0.60)	8.18	1.53	0.64	0.76	48.80	38.96	0.50		
NHL3.5 RM	66.41 (0.35)	0.15 (0.00)	5.39 (0.03)	1.16 (0.01)	0.83 (0.00)	1.08 (0.01)	4.86 (0.03)	–	20.12 (0.55)	10.54	2.52	1.42	1.04	46.00	36.54	0.70		
NHL5 RM	62.98 (0.68)	1.64 (0.02)	6.28 (0.07)	2.97 (0.03)	–	8.22 (0.09)	10.57 (0.11)	1.54 (0.02)	5.80 (0.13)	14.54	4.00	1.90	1.29	41.99	34.17	1.06		

Sample	Mineralogical composition (wt%)													
	Lime	Petriflase	Portlandite	disordered	Calcite	C2S	C3S	C3A	C4AF	Wollastonite	C2AS	Bredigite	Quartz	Amorphous
NHL2 C	40.96 (0.19)	0.66 (0.00)	0.66 (0.00)	0.66 (0.00)	1.89 (0.01)	20.46 (0.09)	0.82 (0.00)	2.32 (0.01)	3.17 (0.01)	0.79 (0.00)	–	–	1.00 (0.00)	27.27 (0.45)
NHL3.5C	27.25 (0.12)	1.24 (0.01)	1.30 (0.01)	1.30 (0.01)	1.58 (0.01)	39.21 (0.17)	0.89 (0.00)	3.61 (0.02)	9.03 (0.04)	0.33 (0.00)	–	–	0.12 (0.00)	15.45 (0.49)
NHL5 C	14.96 (0.07)	1.45 (0.01)	0.85 (0.00)	0.85 (0.00)	3.16 (0.02)	45.56 (0.22)	0.65 (0.00)	0.97 (0.00)	9.37 (0.05)	–	1.88 (0.01)	6.48 (0.03)	0.17 (0.00)	14.53 (0.55)

inserting a temperature sensor into the lime powder. The lime remained in the form of powder during the entire slaking process. After the stabilization of the temperature NHL samples were stored in plastic sealed bags in order to prevent further carbonation.

2) *Passive slaking* (PS), by curing the NHL quicklimes in ventilated boxes at low ( $60 \pm 5\%$  RH, PS60) and high ( $80 \pm 5\%$  RH, PS80) relative humidity.

The ventilated box is a plastic container measuring 50.5 (L) × 34.5 (W) × 34.5 (H) cm<sup>3</sup>, equipped with an internal grid tray that prevents direct contact between the samples and water. Water placed at the bottom of the box helps maintain the desired relative humidity (RH), which is continuously monitored by a digital controller (Proinstruments, model STC-3028). This controller operates within a temperature range of approximately  $-20\text{ }^{\circ}\text{C}$  to  $+80\text{ }^{\circ}\text{C}$  and an RH range of 0–100 %, with an accuracy of  $\pm 1\text{ }^{\circ}\text{C}$  and 0.1 % RH. To maintain constant humidity, the controller is connected to an 8 cm diameter, 12-V fan. When the measured RH exceeds the setpoint, the fan activates to extract humid air and allow the influx of drier air, and vice versa when the RH drops below the set value. CO<sub>2</sub> concentration inside the box was around  $900 \pm 50$  ppm, and was monitored by means of a CO<sub>2</sub> monitor for indoor air from Temtop (UK), which works in a CO<sub>2</sub> range of 400–5000 ppm with a resolution of 1 ppm and an accuracy of 40 ppm + 5 %.

The choice of exposing the quicklime to CO<sub>2</sub> during slaking was due to simulate industrial conditions during slaking and storage.

X-Ray Diffraction (XRD) was performed on the raw materials, after calcination and during slaking at different intervals until the maximum CaO consumption was reached. An X’Pert Pro Diffractometer with continuous sample rotation system and the disordered crystalline powder method was used. The experimental conditions were: voltage of 45 kV; current of 40 mA; CuK $\alpha$  radiation ( $\lambda = 1.5405\text{ \AA}$ ); explored area between  $4^{\circ}$  and  $70^{\circ} 2\theta$ ; and goniometer speed of  $0.1^{\circ} 2\theta/s$ . Based on the Rietveld method [51], 20 wt% of ZnO was added to the powders as an internal standard to enable a precise quantification of the different crystalline and amorphous phases, previously identified by the X’Pert HighScore Plus 3.0 software by Panalytical. The qualitative reconstruction of mineral profiles was carried out through comparison with PDF databases from the International Centre for Diffraction Data (ICDD). Quantitative phase analysis (QPA) was carried out by means of the TOPAS software (Bruker AXS, Karlsruhe, Germany).

After slaking, samples were carbon-coated and studied with a high-resolution field emission scanning electron microscope (HR-ESEM, FEI model Quanta 400) with EDS microanalysis (Bruker xFlash 6/30 detector) to observe the morphological and textural characteristics of the crystalline and amorphous phases.

Chromatic parameters of the CIELAB system (L\* or lightness, a\* red-green coordinate and b\* yellow-blue coordinate) of the manufactured NHLs were also measured using a Konica Minolta CM-700d/600D spectrophotometer with a CM-S100W DATA Software COLOR SpectraMagic NX.

## 2.2. Preparation and study of the mortars

All mortars were prepared with a CEN standard sand (of siliceous composition), in a binder-to-sand ratio of 1:3 by weight, according to EN 196-1:2016 [52], but modifying the amount of kneading water to obtain flow values of 150–156 mm, corresponding to a workable consistence of the mortar fresh paste, within the range established by the standard EN 1015-6:1998 [53] (140–200 mm). The flow values were measured following the flow table test (EN 1015-3:1999 [54]). The bulk density of the fresh mortar pastes (kg/m<sup>3</sup>) was also measured by the volumetric method (EN 1015-6:1998 [53]). The precise amounts of the mortar components, as well as the consistence and bulk density values are reported in Table 1.

Three mortars specimens were prepared for each NHL and slaking condition, with a total of 27 mortars samples. For the first 7 days in the mould, the specimens were kept at a RH of  $95 \pm 5\%$  and, after

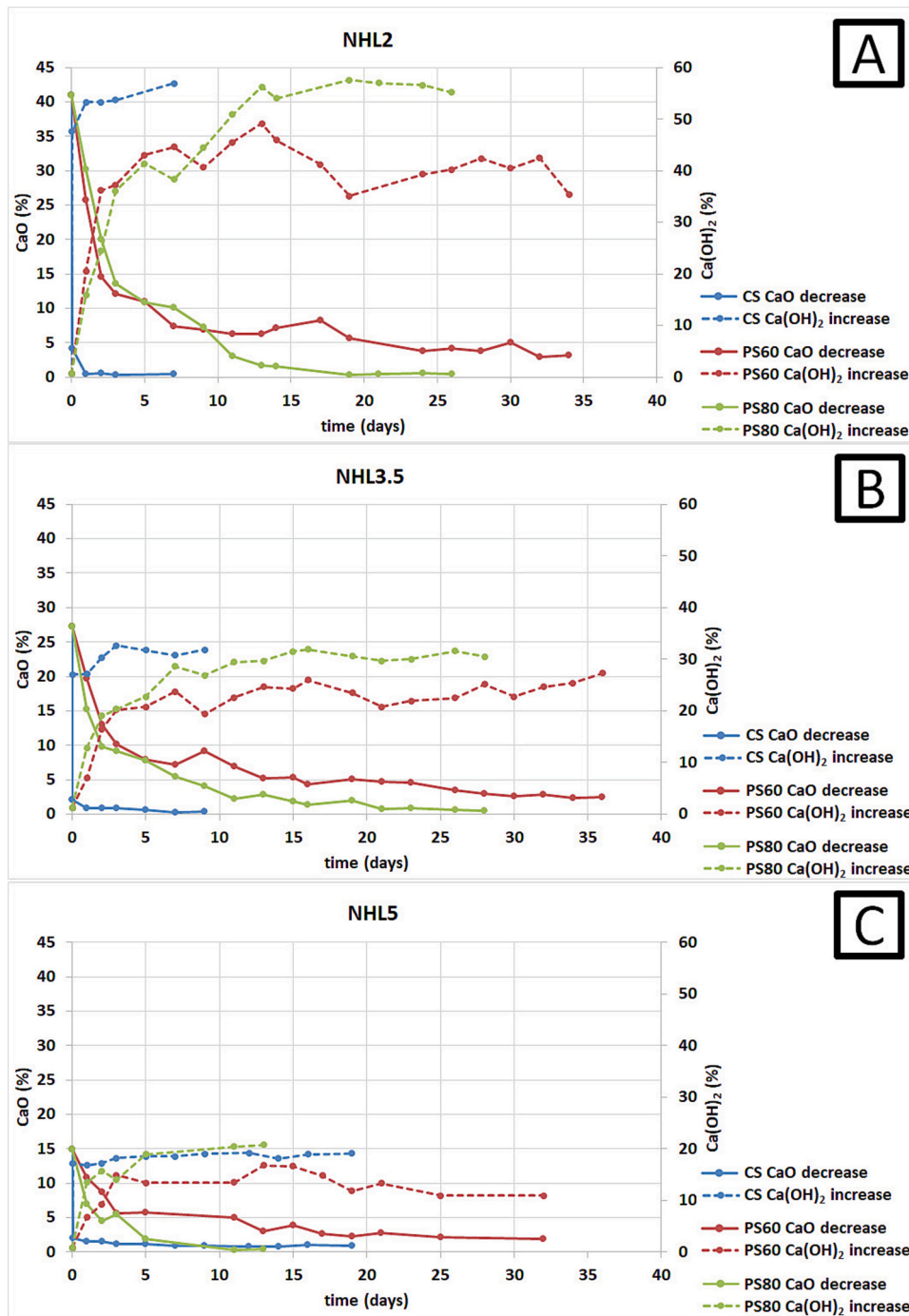


Fig. 1. Evolution of the CaO and Ca(OH)<sub>2</sub> during conventional (CS) and passive slaking at 60 % (PS60) and 80 % RH (PS80) of NHL2 (A), NHL3.5 (B) and NHL5 (C).

demoulding, they were exposed to a RH of 65 ± 5 % for the following 21 days. Temperature was kept stable at 20 ± 2 °C during the whole curing period.

The determination of the mechanical flexural and compressive strengths of the mortars after 28 days of curing was carried out according to the EN 1015-11:2019 standard [55], using a MATEST hydraulic press model E181 with double frame 25KN/300KN. The test was carried out on the 3 standardized specimens of 4 × 4 × 16 cm of each mortar.

X-Ray diffraction Quantitative Phase Analysis (XRD-QPA) was carried out on mortar samples at 28 days. Prior to the analysis, the coarser fraction was separated using a sieve with a mesh size of 0.100 mm. XRD analyses and QPA were performed with the same measurement

conditions and software as those mentioned above.

A petrographic characterization was also performed on mortar samples according to the EN 12407:2007 standard [56]. The equipment used was a Carl Zeiss “Jenapol-U” polarized light optical microscope (POM) equipped with a digital camera (Nikon D7000) and the thin sections were half stained with alizarin to distinguish calcite from dolomite.

**Table 3**  
Final mineralogical composition of the limes slaked under the three different methods (estimated standard deviations are in brackets). CS: conventional slaking; 60PS: passive slaking at 60 % ± 5 % RH; PS80: passive slaking at 80 ± 5 % RH.

Sample	Lime	Periclase	Ord. Portl.	Dis. Portl.	Calcite	C2S	C3S	C3A	C4AF	CS	C2AS	Bredigite	Hydro-garnet	CACH	Quartz	Amorphous
NHL2 CS (7d)	0.24 (0.00)	0.78 (0.01)	36.57(0.32)	18.12 (0.16)	3.17 (0.03)	19.85(0.17)	0.23 (0.00)	1.09 (0.01)	0.90 (0.01)	0.73 (0.01)	-	-	5.26 (0.05)	3.97 (0.04)	0.37 (0.00)	8.70 (0.10)
NHL2 PS60 (34d)	3.23 (0.03)	0.81 (0.01)	7.71 (0.06)	27.84 (0.21)	17.11 (0.13)	21.51(0.16)	0.29 (0.00)	1.37 (0.01)	2.65 (0.02)	0.58 (0.00)	-	-	-	1.20 (0.01)	1.02 (0.01)	14.69 (0.85)
NHL2 PS80 (26d)	0.35 (0.00)	0.72 (0.01)	19.20 (0.21)	36.94 (0.41)	2.90 (0.03)	19.27(0.21)	0.81 (0.01)	0.74 (0.01)	1.30 (0.01)	0.85 (0.01)	-	-	-	3.34 (0.04)	0.70 (0.01)	12.90 (0.12)
NHL3.5 CS (9d)	0.41 (0.00)	0.77 (0.01)	25.08 (0.20)	7.53 (0.06)	2.27 (0.02)	32.03 (0.26)	1.78 (0.01)	0.69 (0.01)	0.61 (0.01)	0.87 (0.01)	-	-	8.67 (0.07)	5.57 (0.05)	0.05 (0.00)	13.68 (0.89)
NHL3.5 PS60 (36d)	2.62 (0.03)	1.12 (0.01)	6.95 (0.08)	18.60 (0.21)	10.35 (0.12)	36.32(0.42)	0.33 (0.00)	2.43 (0.03)	5.45 (0.06)	0.15 (0.00)	-	-	-	0.86 (0.01)	0.26 (0.00)	14.50 (0.13)
NHL3.5 PS80 (28d)	0.53 (0.01)	0.93 (0.01)	11.58(0.10)	17.90 (0.15)	3.77 (0.03)	32.54(0.28)	0.97 (0.01)	0.87 (0.01)	2.96 (0.03)	0.28 (0.00)	-	-	-	6.99 (0.06)	0.20 (0.00)	20.47 (0.90)
NHL5 CS (19d)	0.98 (0.01)	1.45 (0.01)	2.96 (0.02)	16.55 (0.11)	1.31 (0.01)	40.93 (0.27)	3.52 (0.02)	1.44 (0.01)	1.27 (0.01)	0.00	0.55 (0.00)	3.05 (0.02)	10.57 (0.07)	5.25 (0.04)	0.08 (0.00)	10.09 (0.76)
NHL5 PS60 (32d)	1.85 (0.01)	1.16 (0.01)	2.42 (0.01)	8.48 (0.05)	14.79 (0.09)	39.11(0.23)	2.88 (0.02)	1.04 (0.01)	1.45 (0.01)	-	0.97 (0.01)	4.91 (0.03)	-	2.53 (0.02)	0.12 (0.00)	18.29 (0.62)
NHL5 PS80 (13d)	0.08 (0.00)	1.19 (0.01)	3.25 (0.02)	18.78 (0.12)	1.95 (0.01)	32.97(0.21)	3.57 (0.02)	0.95 (0.01)	0.32 (0.00)	-	1.09 (0.01)	2.15 (0.01)	5.37 (0.03)	9.09 (0.06)	0.12 (0.00)	19.12 (0.67)

### 3. Results and discussion

#### 3.1. Chemical and mineralogical composition of raw (RM) and calcined (C) materials

The chemical and mineralogical analysis of the sampled stones was carried out to corroborate their suitability as raw materials for the manufacture of the three types of NHL. As shown in Table 2, their composition is mainly calcitic, although all of them contain also variable amounts of dolomite (0.15–1.99 %). The lower the hydraulic degree of the NHL, the higher the amount of calcite in the corresponding raw material, to provide the final amount of free lime (Ca(OH)<sub>2</sub>) required by the EN 459–1:2015 standard [57]. The quartz and the plagioclase content are approximately 5–10 % and 1–3 %, respectively. The clay content and type are important factors to consider, as they greatly influence the type of silicates and aluminates formed [34,58,59]. The NHL2 raw material only presents 2 % of clays of the illite variety ((K,H<sub>3</sub>O)(Al, Mg, Fe)<sub>2</sub>(Si, Al)<sub>4</sub>O<sub>10</sub>), while the rest of the samples present between 6 and 19 % of clays of the illite and kaolinite (Al<sub>2</sub>Si<sub>2</sub>O<sub>5</sub>(OH)<sub>4</sub>) type. The amorphous content is variable and can be associated with the paracrystalline fraction of the clays [6].

The CI calculated for the three raw materials (Table 2) is always the highest value of the range established for each type of NHL (0.3–0.5 for NHL2, 0.5–0.7 for NHL3.5, 0.7–1.1 for NHL5). The loss of ignition values (LOI, Table 2), related with the loss of carbonates and structural water, coincide with the weight loss calculated after calcination, which is 39 % for NHL2, 36 % for NHL3.5 and 35 % for NHL5, all values very close to those reported for marly limestones by Vola et al. [10].

In accordance with other authors [5,47], quicklime (CaO) and dicalcium silicate (C<sub>2</sub>S) are the main crystalline phases present in the calcined products (Table 2), with variable content depending on the raw material composition. NHL2 C (C stands for calcined), with feebly hydraulic degree, presents more lime (CaO) than C<sub>2</sub>S, due to the higher initial CaCO<sub>3</sub> content. While in the rest of the samples (NHL3.5C and NHL5 C), C<sub>2</sub>S is the major phase, as the siliceous phases (expressed as SiO<sub>2</sub> content) are predominant in the raw materials. Lime (CaO), periclase (MgO) and portlandite (Ca(OH)<sub>2</sub>) have been detected in all calcined materials. The latter formed due to exposure of the calcined samples to the laboratory relative humidity during handling [5,6,60]. This was expected as lime is a thermodynamically unstable product that tend to react with air water vapour, sometimes forming a thin layer of calcium hydroxide on the surface of the lime particles [22].

According to the XRD-QPA results, the portlandite detected in all calcined samples is disordered or poorly crystalline. The presence of amorphous phases in portlandite precursors and carbonation products has already been found in aerial lime [6,61–66] and cement [67–70]. Rodriguez-Navarro et al. [66], particularly, demonstrated that portlandite is not governed by a classical crystallisation, as an amorphous calcium hydroxide (ACH) forms as a precursor of crystalline portlandite.

Periclase (MgO), frequently detected in laboratory-obtained limes with hydraulic properties [5,10,12,71] comes from the calcination of Mg-bearing phases in the raw materials, such as illite and dolomite. The presence of magnesium is known to decrease the reactivity of quicklime [14,71,72], which is believed to be one of the reasons for the indirect relationship sometimes found between the size of quicklime crystallites and their reactivity [71,73].

Other non-hydraulic phases detected in the calcined products but pre-existing in the raw materials are calcite and quartz. The presence of calcite (0.10–3.16 %) may be due to different reasons: 1) partial carbonation of the formed portlandite, 2) re-carbonation of CaO inside the kiln (back-reactions [1,6,22,50,60,74]) and/or 3) incomplete thermal decomposition during calcination.

Quartz has been found in traces (0.07–1 %) after calcination, indicating that almost all microcrystalline quartz present in the raw materials was reactive under calcination, as previously found [6].

Dicalcium silicate (C<sub>2</sub>S, 2CaO·SiO<sub>2</sub>), under the form of larnite

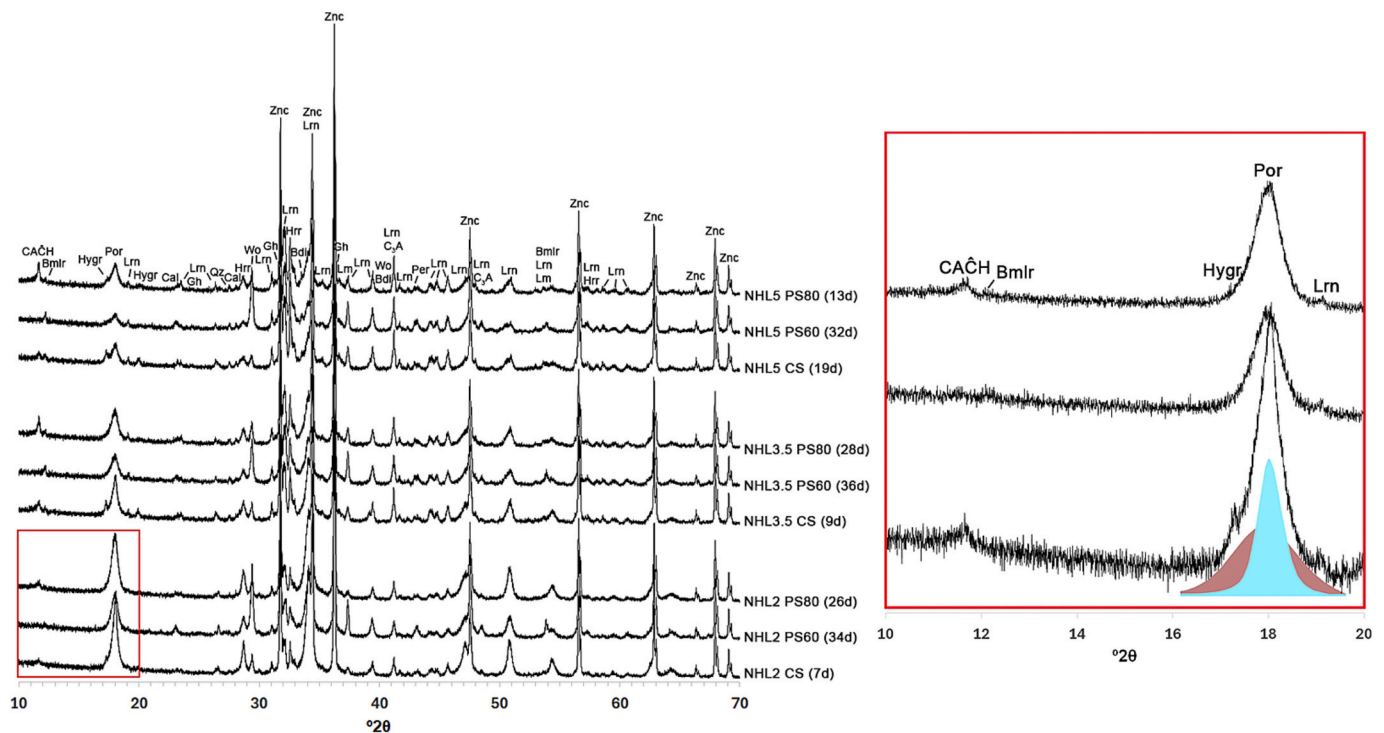


Fig. 2. X-ray diffraction patterns of the range 10–70 °2θ of the last study interval of the slaked samples. A zoomed-in view (red rectangle) of the 10–20 °2θ region is shown for the diffractograms of slaked NHL2 samples, including the diffraction reflex of portlandite's (001) basal plane highlighted in maroon (disordered portlandite) and cyan (ordered portlandite). CS: Conventional slaking; PS60: Passive slaking at 60 ± 5% RH; PS80: Passive slaking at 80 ± 5% RH. Numbers in brackets refer to the day of analysis from the start of slaking. According to Warr [92]: Bdi: Bredigite, Bmlr: Brownmillerite, Cal: Calcite, Gh: Gehlenite, Hrr: Hatrurite, Lrn: Larnite, Lm: Lime, Per: Periclase, Por: Portlandite, Qz: Quartz, Wo: Wollastonite, Znc: Zincite. CAĈH: Monocarboaluminate, C3A: Tricalcium aluminate (celite) and Hygr: Hydrogarnet.

$\beta$ - $\text{Ca}_2\text{SiO}_4$  [75], the most stable polymorph at room temperature [76], was found as the main hydraulic phase in all calcined products. Tricalcium silicate ( $\text{C}_3\text{S}$ ,  $3\text{CaO}\cdot\text{SiO}_2$ ) was found in amounts lower than 1 %, under the form of monoclinic hatrurite ( $\text{Ca}_3\text{SiO}_5$ ) [77]. Its presence is explained by the existence of hot spots in the kiln [63,78] that reach temperatures above 1250 °C [12], which trigger the combination of  $\text{C}_2\text{S}$  with CaO to form  $\text{C}_3\text{S}$  [5].

Other minor hydraulic phases found are tricalcium aluminate (cubic  $\text{C}_3\text{A}$  [79],  $3\text{CaO}\cdot\text{Al}_2\text{O}_3$ ), tetra-calcium aluminoferrite or felite ( $\text{C}_4\text{AF}$ ,  $4\text{CaO}\cdot\text{Al}_2\text{O}_3\cdot\text{Fe}_2\text{O}_3$ ), also known as brownmillerite ( $\text{Ca}_2(\text{Al},\text{Fe})_2\text{O}_5$ ), here refined according to the structure of Colville & Geller [80], and gehlenite ( $\text{Ca}_2\text{Al}(\text{SiAl})\text{O}_7$ ,  $\text{C}_2\text{AS}$ ,  $2\text{CaO}\cdot\text{Al}_2\text{O}_3\cdot\text{SiO}_2$ ), the latter only found in NHL5 calcined product. These phases have originated from the plagioclases, k-feldspars, illite and kaolinite clays, and ilmenite of the raw materials, as suggested by Kozlovcev & Prikryl [60] and Kozlovcev & Válek [12].

Other phases found in the calcined materials are wollastonite (CS,  $\text{CaSiO}_3$ ) and bredigite ( $\text{Ca}_7\text{Mg}(\text{SiO}_4)_4$ ), both non-hydraulic or non-hydration-reactive silicates [5,81]. Wollastonite, together with other polymorphs such as pseudowollastonite, is commonly detected in laboratory-made limes [6,12,60] and it is known to have a low hydration activity [82]. The formation of bredigite may be associated with the presence of gehlenite by the decomposition sequence bredigite-gehlenite-diaspore [83]. Even though, its presence in some cement clinkers [84,85] and calcium sulfoaluminate cements (CSA) [86,87] seem to support the hypothesis that its formation may be associated with previous transition compounds such as wollastonite, larnite, merwinite, and calcium-magnesium silicates [88,89].

Finally, the amorphous content in the calcined materials can be attributed to the presence of either low crystalline CaO fraction and highly reactive Ca-rich amorphous material [5], or non-crystalline fraction of calcium hydroxide [63].

### 3.2. Study of the limes during slaking

#### 3.2.1. Evolution of $\text{CaO}$ and $\text{Ca}(\text{OH})_2$ , duration and kinetics of slaking

The mineralogical composition of the limes was monitored during the whole slaking process, until the content of lime (CaO) was considered stable (i.e. no further hydration could be expected). For this reason, the duration of the process has been different according to the slaking method, as it can be observed in Fig. 1, where the decrease in CaO and the increase in  $\text{Ca}(\text{OH})_2$  have been plotted over time. All samples showed a decrease in the lime content during hydration, although with a different kinetics depending on the slaking method used. Under conventional slaking the hydration of calcium oxide is faster, as CaO was almost totally consumed after only 1 day, compared with both procedures of passive slaking, in which the minimum content of CaO was reached after the first 15 days. The slaking rate calculated after one day from the linear coefficient of the CaO decrease curve (Fig. SM1) was indeed 3–4 times higher in conventional slaking than in the passive one.

As expected, during conventional slaking, the limes with the highest CaO content reached the highest temperature (95–96 °C for NHL2 and NHL3.5 and 83 °C for NHL5) (Fig. SM2). The temperature decreases in NHL3.5 and NHL5, on the other hand, was more gradual, remaining above 40 °C for 1–2 h, whereas in NHL2, it lasted only 20 min.

Conventional slaking (CS) and passive slaking at 80 % of relative humidity (PS80) were considered completed when the content of lime (CaO) was almost null in all the NHLs (Table 3). Notwithstanding, in the NHLs slaked under 60 % of RH (PS60), slaking was stopped even though a residual content of lime (2.5 % in average, Table 3) was still present in the three NHLs.

The reason why slaking at 60 % was considered concluded before CaO reached 0 %, is related with the fact that the portlandite formed from the hydration of calcium oxide was undergoing carbonation under the conditions used for passive slaking, and therefore its content did not

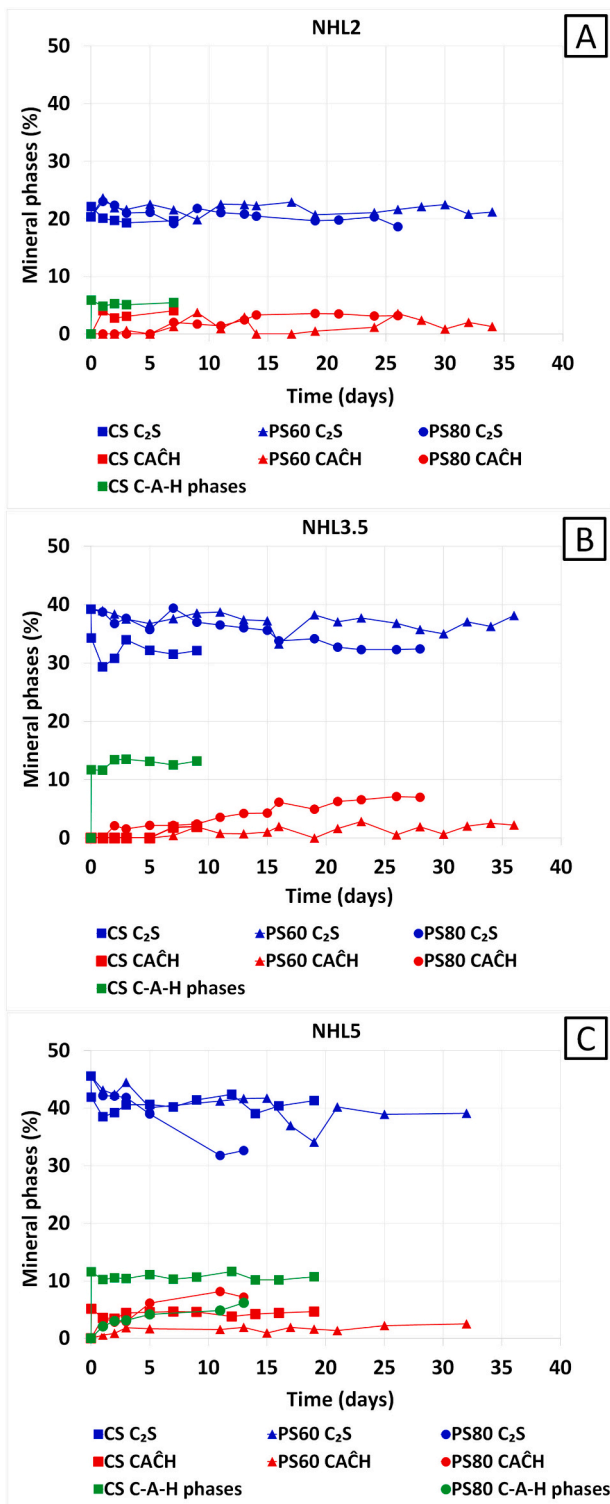


Fig. 3. Evolution trend of the main mineral phases under conventional slaking (CS) and passive slaking at  $60 \pm 5\%$  RH (PS60) and  $80 \pm 5\%$  RH (PS80) of NHL2 (A), NHL3.5 (B) and NHL5 (C).  $C_2S$ : dicalcium silicate, C-A-H: hydrogarnet/hydrocalumite, CAĤH: monocarboaluminate.

increase uniformly over time but, instead, tended to stabilise (as in the case of NHL2 and NHL3.5 under PS60, Fig. 1) or even decrease (in NHL5 under PS60, Fig. 1). Indeed, the calcite content found at the end of the slaking process was always higher in the NHLs slaked under 60 % of relative humidity (PS60, Table 3), where it reached  $\sim 14\%$  in average, compared to the other NHLs, where calcite was between 1.3 and 3.8 %

(CS and PS80, Table 3). It is worth noting that only calcite, not its polymorphs, have been found here, as expected considering that it is the most stable polymorph, from RH higher than 40 % [90].

Knowing that air slaking and recarbonation significantly decrease the slaking capacity of the quicklime [31], the passive slaking at 60 % was concluded before CaO was totally consumed.

Although uneven hydration was minimised by periodically stirring the lime powders, the presence of a residual content of CaO can also be ascribed to the presence of lime lumps, in which the formation of a superficial layer of calcium hydroxide may have prevented complete transformation of the oxide [17,91].

The duration of passive slaking at 80 % (13–28 days) and 60 % RH (32–37 days) matches the time intervals estimated by Dai [25] under the *windslaking* method at open (21 days) and indoor air (40 days). This suggests that the role of wind and/or water mist in an open environment resembles high relative humidity conditions in indoor air.

Either in conventionally and passively slaked limes, two populations of crystalline portlandite, an ordered and a disordered one, were found by XRD-QPA (Table 3). The presence of two distinct portlandite populations with differing structural order is clearly visible in the inset of Fig. 2 and is further supported by their crystallite size differences: the ordered portlandite (highlighted in maroon in Fig. 2) averages 25–50 nm, while the disordered one (highlighted in cyan in Fig. 2) ranges from 12 to 20 nm at the end of the slaking process (as shown in SM3).

The amount of ordered portlandite is always higher under conventional slaking (CS) (Table 3). Under passive slaking (PS60 and PS80), instead, the amount of disordered portlandite is always higher than the ordered one, with the only difference that at higher humidity (PS80), the amount of the latter increases (Table 3). This can be explained by the initial formation of a precursor amorphous calcium hydroxide (ACH, [66]), whose transformation into ordered portlandite is conditioned by the amount of available water in the environment, and therefore by the degree of hydration of the lime, which is lower in the limes slaked at 60 % of relative humidity (PS60). The presence of the double population of portlandite has been previously detected, as commented above, although how this influences the reactivity of the lime towards carbonation is so far unknown.

Under the experimental conditions of this study, periclase (MgO) has not suffered hydration neither into brucite ( $Mg(OH)_2$ ), nor in its pre-hydration precursors, as the periclase content at the end of slaking (Table 3) is similar to that in the calcined products (Table 2). This is not surprising, considering the low reactivity towards water (and therefore the slow rehydration kinetics) of this oxide, compared to CaO [16,93].

### 3.2.2. Influence of slaking on the hydration of silicate and aluminate phases

Even though the only transformation expected in limes during slaking is the hydration of the calcium (and magnesium) oxide, this work explores also the effect that the addition of water (both in the liquid (CS) and vapour state (PS60 and PS80)) might have on the other phases constituting natural hydraulic lime, in particular the silicate and aluminate phases.

As far as the hydration of silicate phases is concerned, mainly non-crystalline or amorphous C-S-H can be expected if any [48], as no crystalline C-S-H has been detected neither during (Fig. 3) nor at the end of slaking (Table 3). Even though it seems that there is a slightly bigger decrease of the  $C_2S$  content during conventional (CS) and passive slaking at high RH (PS80) (Fig. 3), this is not straightforward, as the observed variations might be related to samples heterogeneity.

The only hydrated phases clearly identified in some of the slaked limes are hydrogarnet ( $Ca_3(Al_xFe_{1-x})_2(SiO_4)_y(OH)_{4(3-y)}$ ) [94] and monocarboaluminate (CAĤH), the latter present in all slaked limes. Both phases come from the fast hydration of  $C_3A$  and  $C_4AF$  [48], whose content has decreased in all NHLs, compared to the calcined products (Table 2), especially under conventional slaking.

Hydrogarnet, found in all the NHLs that underwent conventional slaking in amounts from 5 to 10 %, as well as in NHL5 (the most

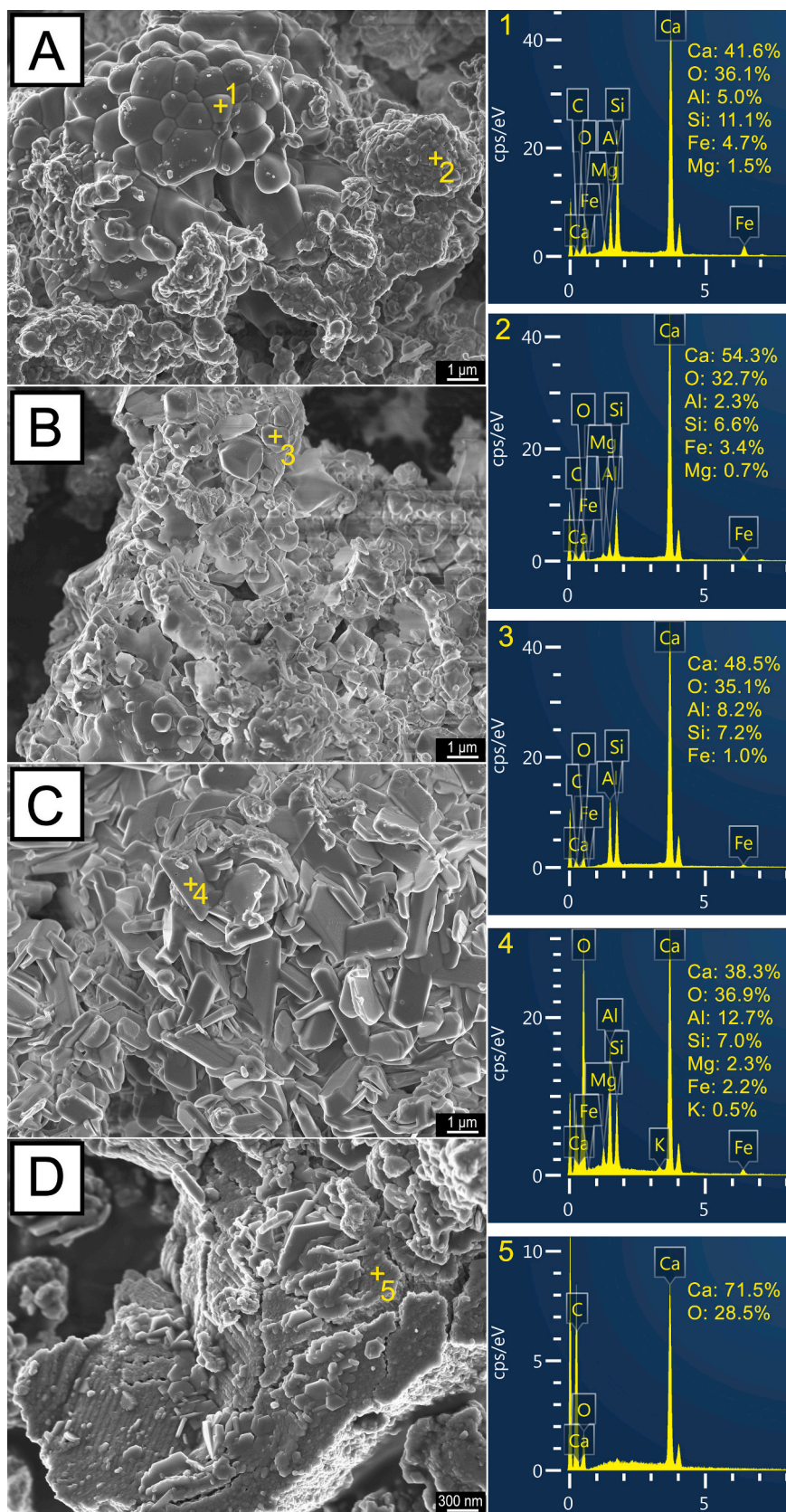


**Fig. 4.** HR-ESEM images of: A) NHL3.5 CS, agglomerate of calcium-silicate particles with globular (EDS spectrum marked with +1) and irregular morphologies (EDS spectrum marked with +2); B) NHL5 CS, agglomerate of hydrogarnet particles with cubic habit (EDS spectrum marked with +3); C) NHL5 PS80, silico-aluminate tabular to prismatic particles (EDS spectrum, marked with +4); D) NHL2 PS60, calcic agglomerate with hexagonal platelets of portlandite (EDS spectrum marked with +5).

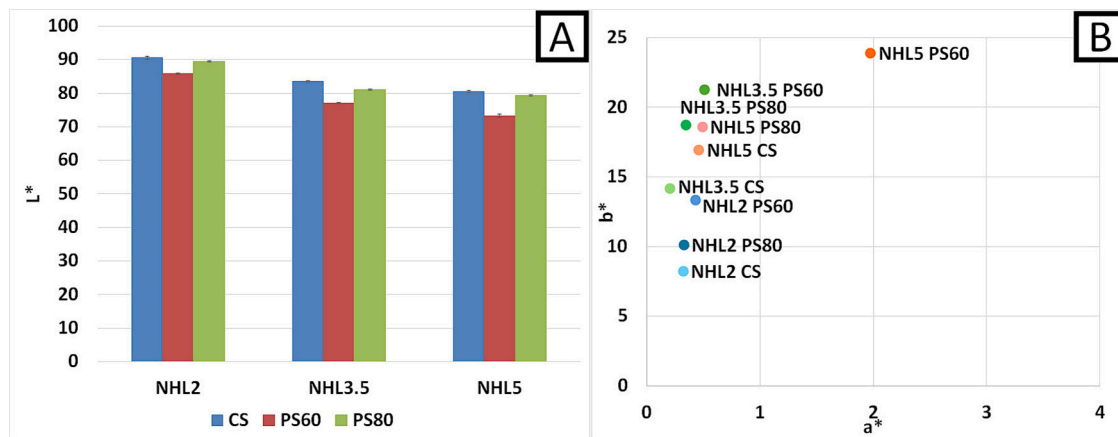


Fig. 5. Graphical representation of A: the lightness values ( $L^*$ ) and B: the colour parameters  $b^*$  versus  $a^*$  of the limes hydrated with the different slaking methods. CS: conventional slaking; PS60: passive slaking at  $60 \pm 5\%$  RH; PS80: passive slaking at  $80 \pm 5\%$  RH.

hydraulic one) slaked under high relative humidity (PS80), is the crystalline form of hydrated calcium aluminates (C-A-H) [16,48,95,96]. Less stable hydrated calcium aluminate phases are those of the hydrocalumite-hydroalcite-pyroaurite family, also known as AFm phases [95,97–100]. These phases were detected during slaking monitoring (Fig. 3), especially hydrocalumite ( $\text{Ca}_4\text{Al}_2(\text{Cl},\text{CO}_3,\text{OH})_2(\text{OH})_{12}\cdot 4\text{H}_2\text{O}$ ), but none of them was present at the final slaking interval, likely because of their transformation into monocarboaluminate, or into the most stable hydrogarnet [48]. Other less stable AFm phases that could have been present during the slaking process but that were not detected here, are hydroxy-AFm, hemicarboaluminate or strätlingite, also called gehlenite hydrate [95,100].

### 3.2.3. Microstructure and colour of slaked limes

SEM analyses were performed in order to observe possible changes in the microstructure of NHLs depending on the slaking method. This technique also made it possible to identify the different morphologies of some of the phases previously detected by XRD.

All limes show agglomerates of 10–30  $\mu\text{m}$  composed of sub-micrometric particles (0.05–2  $\mu\text{m}$ ) of globular and irregular morphologies (Fig. 4A). Their chemical composition (EDS spectra 1 and 2 in Fig. 4) indicates that they are calcium silicates with small amounts of aluminum, iron, and magnesium. In particular, the globular particles (Fig. 4A, Spectrum 1) could be larnite ( $\text{Ca}_2\text{SiO}_4$ ,  $\text{C}_2\text{S}$ ), whilst the irregularly shaped particles could correspond, according to the EDS spectra (Fig. 4A, Spectrum 2), to alite ( $\text{Ca}_3\text{SiO}_5$ ,  $\text{C}_3\text{S}$ ), both coexisting with iron-bearing phases such as brownmillerite.

In the more hydraulic limes (NHL3.5 and NHL5), AFm or C<sub>4</sub>AH phases are also present forming agglomerates of particles with typical morphologies [101]. In NHL5, particles of 0.5–1  $\mu\text{m}$  with a cubic habit typical of hydrogarnet (Fig. 4B, Spectrum 3), and crystals of tabular to prismatic habit (1–2  $\mu\text{m}$ ) (Fig. 4C) were also detected. The latter present a silico-aluminate composition (Spectrum 4 in Fig. 4) that can correspond to gehlenite ( $\text{Ca}_2\text{Al}(\text{SiAl})\text{O}_7$ ), a phase previously detected by XRD, or to another phase of the calcium aluminate-silicate system.

The less hydraulic limes (NHL2) contain less particle agglomerates of calco-silicate composition, as particles of  $\text{CaO-Ca}(\text{OH})_2$  prevail (Fig. 4D, Spectrum 5). Thin hexagonal platelets of portlandite of  $\sim 1\ \mu\text{m}$  (Fig. 4D) grow on the surface of bigger agglomerates (up to 30  $\mu\text{m}$ ) that present fissures attributable to the hydration of CaO. The limes also display inherited structures in the uncalcined relics, such as pores (A and B in SM4) and fracture planes characteristic of quartz fragments (C in SM4).

Fig. 5 shows how the mineralogical changes resulting from different slaking methods influence the colour of the NHLs produced. In general, limes slaked using the conventional method exhibit the highest lightness values ( $L^*$ ) and the lowest  $a^*$  and  $b^*$  values (SM5), which can be

attributed to their high portlandite content. In contrast, limes slaked under the passive method at lower relative humidity (PS60) appear less luminous due to the reduced development of this phase (as shown in Table 3). Therefore, a higher degree of hydration and portlandite content results in a whiter final product, whereas an increased content of hydraulic phases imparts brownish tones to the binders.

### 3.3. Study of mortars

#### 3.3.1. Mineralogical composition

Calcium oxide (lime) was not detected in any of the studied mortars, by contrast, periclase was still detected in amounts ( $\sim 1\%$ , Table 4) similar as those found in the slaked limes (Table 3). Once more, brucite ( $\text{Mg}(\text{OH})_2$ ) was not detected, either because magnesium oxide did not transform into its crystalline hydrated form, or due to the overlapping of the peaks of these phases in the X-ray diffraction pattern.

A general trend that can be observed in the NHL2 and NHL3.5 mortars, is that a highest amount of ordered portlandite is formed compared to the corresponding slaked limes, indicating that curing induced a higher degree of crystallinity of this phase.

If comparing the initial amounts of total portlandite (ordered and disordered) and calcite in the slaked limes (Table 3) with those found in the mortars after 28 days of curing (Table 4 and SM6), it is not possible to see a clear trend of carbonation, as those amounts remain similar, and the little variations might be due to samples heterogeneity. Therefore, carbonation in NHL mortars is still very low after 28 days, as also found in other research [102–107]. Among all the samples, NHL5 mortars show in average the lowest degree of carbonation, even though the presence of amorphous calcite cannot be discarded either in all of them.

As far as the  $\text{C}_2\text{S}$  content is concerned, it can be observed that it has decreased by 8–10 % in NHL2 mortars, by 6–10 % in NHL3.5 mortars, and by 4–10 % in the NHL5 ones, compared to the initial amounts in the slaked limes. This decrease in the  $\text{C}_2\text{S}$  content is related to its hydration to form C-S-H. Even though no crystalline C-S-H has been detected, the higher amorphous content in all the mortars compared to the limes can be related to the formation of amorphous C-S-H. This would confirm that hydration is already occurring at early ages in NHL mortars. Overall, the  $\text{C}_2\text{S}$  after 28 days of mortars curing is in comparable amounts independently on the slaking different method.

Other hydraulic ( $\text{C}_3\text{S}$ ,  $\text{C}_3\text{A}$ ,  $\text{C}_4\text{AF}$  and  $\text{C}_2\text{AS}$ ) and non-reactive phases (wollastonite and bredigite) hardly show any variation in their amounts. Approximately 2 % of quartz has been detected in the mortars, as a residual fraction of the sand that could have remained despite separation of the aggregate prior to the XRD analysis.

Hydrocalumite was found in NHL3.5 and NHL5 mortars only when the lime was slaked at 60 % relative humidity (PS60). This occurs

**Table 4**  
Mineralogical composition of the mortar samples (M) prepared with limes slaked under the different 3 methods (estimated standard deviations are in brackets). CS: conventional slaking; 60PS: passive slaking at 60% ± 5% RH; PS80: passive slaking at 80 ± 5% RH.

Sample	Periclase	Ord. Portl.	Dis. Portl.	Calcite	C2S	C3S	C3A	C4AF	CS	C2AS	Bredigite	Hydro-garnet	Hydro-calumite	CAcH	Quartz	Amorphous
M-NHL2 CS	-	37.37 (0.33)	12.05 (0.11)	3.33 (0.03)	11.11 (0.10)	0.82 (0.01)	0.89 (0.01)	0.52 (0.01)	0.93 (0.01)	-	-	4.86 (0.04)	-	4.75 (0.04)	1.96 (0.02)	21.41 (0.93)
M-NHL2 PS60	-	20.67 (0.18)	18.34 (0.16)	15.68 (0.13)	11.86 (0.10)	0.21 (0.00)	0.66 (0.01)	0.82 (0.01)	0.69 (0.01)	-	-	-	-	7.15 (0.06)	2.33 (0.02)	21.60 (0.89)
M-NHL2 PS80	-	31.11 (0.29)	21.99 (0.21)	5.092 (0.05)	10.29 (0.10)	2.48 (0.02)	0.78 (0.01)	0.55 (0.01)	0.84 (0.01)	-	-	3.24 (0.03)	-	7.64 (0.07)	2.26 (0.02)	13.70 (0.10)
M-NHL3.5 CS	0.76 (0.01)	28.02 (0.22)	4.95 (0.04)	2.145 (0.02)	25.96 (0.20)	3.90 (0.03)	0.19 (0.00)	0.77 (0.01)	0.68 (0.01)	-	-	8.75 (0.07)	-	7.07 (0.06)	1.36 (0.01)	15.47 (0.85)
M-NHL3.5 PS60	-	6.27 (0.05)	18.46 (0.15)	12.72 (0.10)	25.33 (0.21)	0.76 (0.01)	0.13 (0.00)	1.62 (0.01)	0.65 (0.01)	-	-	3.47 (0.03)	4.661 (0.04)	7.23 (0.06)	1.88 (0.02)	16.83 (0.88)
M-NHL3.5 PS80	0.80 (0.01)	15.86 (0.13)	11.66 (0.09)	3.79 (0.03)	26.02 (0.21)	0.63 (0.01)	1.02 (0.01)	0.57 (0.01)	0.34 (0.00)	-	-	4.39 (0.04)	-	9.62 (0.08)	1.40 (0.01)	23.89 (0.80)
M-NHL5 CS	1.12 (0.01)	8.63 (0.07)	9.75 (0.08)	2.92 (0.02)	32.48 (0.26)	0.51 (0.00)	0.74 (0.01)	1.73 (0.01)	-	0.54 (0.00)	1.38 (0.01)	10.17 (0.08)	-	7.83 (0.06)	1.36 (0.01)	20.84 (0.83)
M-NHL5 PS60	0.56 (0.00)	1.09 (0.01)	8.45 (0.05)	11.73 (0.06)	30.24 (0.17)	0.52 (0.00)	0.14 (0.00)	1.86 (0.01)	-	1.99 (0.01)	2.22 (0.01)	-	3.05 (0.02)	9.21 (0.05)	1.22 (0.01)	27.73 (0.53)
M-NHL5 PS80	0.85 (0.01)	2.04 (0.01)	17.97 (0.12)	2.82 (0.02)	29.51 (0.19)	3.55 (0.02)	0.03 (0.00)	0.68 (0.00)	-	1.29 (0.01)	3.02 (0.02)	5.83 (0.04)	-	10.07 (0.07)	0.50 (0.00)	21.82 (0.66)

because hydrocalumite formation is favoured in the early hydration stages under highly alkaline conditions (pH > 12), particularly when Ca(OH)<sub>2</sub> is abundant. As mortar curing progresses, the reduction in pH due to carbonation, along with the greater thermodynamic stability of other phases such as hydrogarnet or CACH in less alkaline environments exposed to CO<sub>2</sub>, can drive the transformation of hydrocalumite into other phases.

Hydrogarnet and monocarboaluminate were found unvaried in mortars prepared with conventionally slaked NHLs, whilst an increase in its amount is recorded in the majority of the mortars prepared with passive slaked limes. This may be due to the tendency to form more stable phases at the curing conditions of the mortars, as previously mentioned.

Finally, as in the limes, gehlenite was only detected in NHL5 due to the higher aluminum content in its raw materials. Its content in mortar samples remained stable since it is a phase with low reactivity or slow hydration in contact with water [86,87,108,109].

### 3.3.2. Petrographical characterization

All the studied mortars exhibit, as expected, a fine-grained or microcrystalline calcitic dense matrix. The siliceous aggregate, uniformly dispersed throughout the mortar, consists of mono- and polycrystalline quartz (Qz in Fig. 6A) with a grain size ranging from millimetric to centimetric (well-selected) and subrounded to subangular morphologies (Fig. 6A–D).

Different types of lumps were identified (Fig. 6A–B), the most prevalent ones are remnants of the original rock (or uncalcined relics) that preserve their structure (*under-burnt lumps*, indicated as *Ubt* in Fig. 6A) ranging from 0.5 to 2 mm in size. In contrast, only few *over-burnt lumps* were observed, with a dense vitrified structure, low porosity and a smaller size (0.5–0.7 mm).

The porosity of the matrix is low and mostly vacuolar, meaning it has a rounded morphology (marked with one of the arrows in Fig. 6C). The origin of this type of porosity is attributed to the accumulation of mixing water, which, after the setting and hardening of the mortar, generates these pores, typically found in hydraulic mortars [110]. The fissures (Fig. 6A and C), mostly located within the matrix and surrounding the aggregate grains, can be attributed to the shrinkage that mortars undergo during the drying and hardening phases. The least hydraulic lime (NHL2) shows the highest amount of shrinkage fissures (Fig. 6A–D), due to its higher content in Ca(OH)<sub>2</sub>.

The colour of the matrix, as well as the presence of pores and fissures, is related to the degree of hydraulicity of the lime used. The higher the hydraulic degree, the darker the matrix, as shown in Fig. 6A for M-NHL2 CS and Fig. 6E for M-NHL5 PS90.

At the inner border of pores and fissures, areas with low birefringence colours (grey under cross-polarized light, Fig. 6D) can be observed, primarily attributable to portlandite (Ca(OH)<sub>2</sub>) that has been remobilized during curing (indicated with an arrow in Fig. 6C). This phenomenon of filled fissures occurs predominantly in limes with a lower hydraulic grade, which is logical due to their higher free lime content.

The rounded and angular morphologies typical of di-calcium and tri-calcium silicates, respectively, were not observed in the studied mortars, because the size of C<sub>2</sub>S and C<sub>3</sub>S in NHLs is smaller than those found in historic [78] and/or modern Portland cement mortars [6]. Although at high magnifications, phases containing iron (likely hydraulic) can be observed in the matrix (Fig. 6E–F).

Finally, in the case of the more hydraulic mortars (NHL3.5 and NHL5), a greater irregular porosity along with *lime-lumps* (*Lump* in Fig. 6G–H) of around 1 mm is also observed. These particles are associated with the presence of quicklime (CaO) particles or partially hydrated lime (Ca(OH)<sub>2</sub>) that have not fully reacted with water before being incorporated into the mixture. This incomplete hydration process led to the development of fissures and low-density areas within it. Another notable aspect is the presence of needle- or plate-like phases in

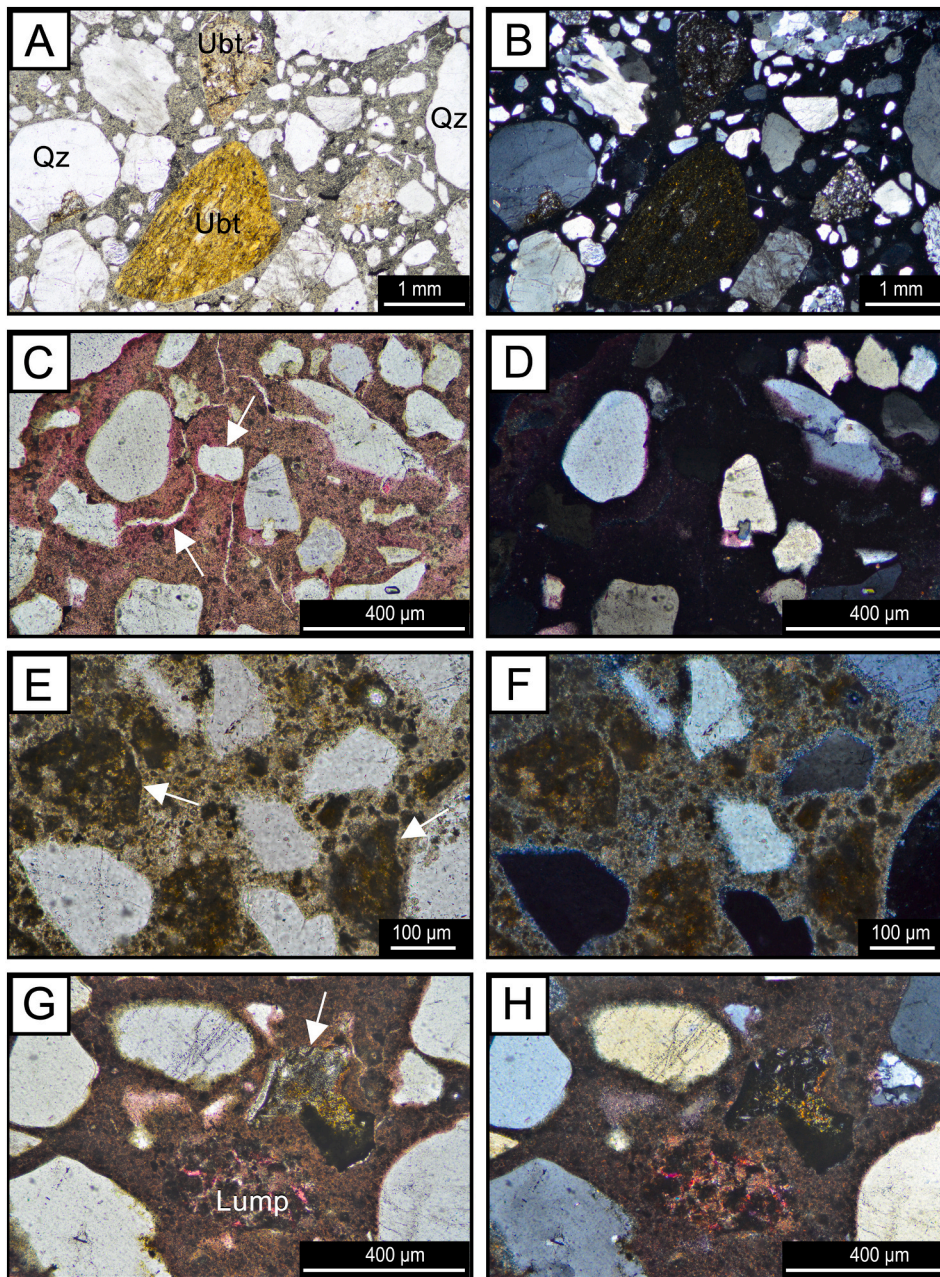


Fig. 6. Polarized light optical microscope (POM) images, in parallel-polarized light (left) and cross-polarized light (right) of: M-NHL2 CS (A-B), M-NHL2 CS(C-D), M-NHL5 PS80 (E-F) and M-NHL3.5 CS (G-H). Qz: Quartz, Ubt: Underbunt-lump, Lump: Lime-Lump.

some of the grains containing iron (marked with an arrow in Fig. 6G–H), which are ascribable to hydraulic phases.

There are no differences observed depending on the slaking method used. All mortars show in general a good adhesion between the aggregate and the matrix, with only few shrinkage fissures appearing along the contact between the grains and the matrix.

### 3.3.3. Mechanical properties and colour

Fig. 7 and SM7 show the mechanical strength values of the mortars after 28 days of curing. It is worth highlighting that the obtained values do not necessarily coincide with the minimum strength values set by the EN 459-1 standard [57], since the water content stipulated by the standard was modified to obtain workable mortar pastes (see Section 2.2, Table 1). However, this does not invalidate the results obtained in this research, as the mechanical data can always be interpreted in terms of the type of lime and the slaking method used.

NHL2 and NHL3.5 mortars whose limes were passively slaked at  $60 \pm 5\%$  RH (PS60) show slightly higher strengths than those made with NHLs slaked conventionally (CS) and at  $80 \pm 5\%$  RH (PS80), while the flexural strength did not reach measurable values in any of the studied mortars. In Pesce et al.'s study [111], it was also concluded that steam-slaked lime mortars exhibit slightly superior strength compared to water-slaked mortars, although those showed an increase in flexural strength.

Theoretically, this could be due to the fact that the hydraulic phases remain in their dehydrated form in the lime at  $60 \pm 5\%$  RH, until it is mixed with water in the mortar, which is when they start reacting with water. This hypothesis seems to be corroborated by the mineralogical data in Table 4, as the decrease in  $C_2S$  content compared to the slaked limes is always higher in the NHLP60 mortars, and this would indicate that the NHLs slaked at a lower relative humidity have a higher reactivity towards hydration when in the mortar. As discussed above

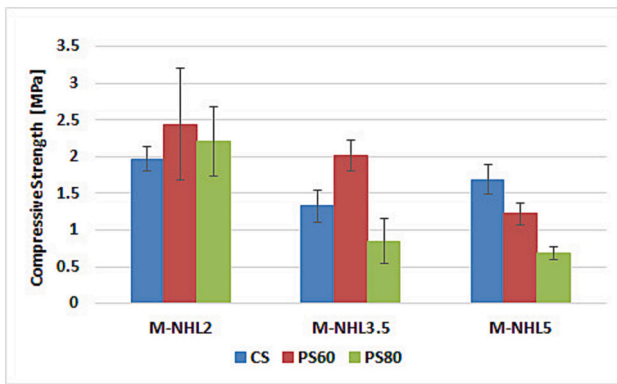


Fig. 7. Compressive strengths (MPa) of the mortars made with the slaked NHLs by the different slaking methods. CS: conventional slaking; PS60: passive slaking at  $60 \pm 5$  % RH; PS80: passive slaking at  $80 \pm 5$  % RH.

(Section 3.3.1), hydration is certainly contributing to the development of strength at this age of the mortar, although carbonation may be the main responsible for the differences found in the mechanical strengths of the mortars after 28 days. It must be noticed, indeed, that the least hydraulic mortars, namely the NHL2 ones, have displayed the highest values of mechanical strength among all the samples studied. Instead, the strength values obtained in the NHL5 mortars are among the lowest ones, and this can be related with the lower carbonation degree of NHL5 mortars, as discussed in Section 3.3.1. Even though the opposite trend should be expected, other studies have also demonstrated that mortar specimens prepared with binders manufactured experimentally in the laboratory do not always show a direct relationship between the content of hydraulic components and the improvement of the mechanical strength [41].

After 28 days of curing (Fig. 8, SM8), the NHL2 mortars showed colour values similar to those of the limes (Fig. 5). The NHL5 mortars, instead, showed higher lightness values ( $L^*$ ) and a higher tendency to yellow shades.

From Fig. 8 it is evident that conventional slaking does have an influence on obtaining lighter or whiter mortars, as long as there is a high percentage of portlandite (as is the case in NHL2 and NHL3.5 mortars). Whereas when the silicate content is high, the lightness of the limes is more dependent on the moisture content of the materials.

#### 4. Conclusions

This research work has explored what occurs to natural hydraulic lime when it is slaked under different methods. Here the conventional slaking, in which water is added in a 1:1 water:CaO ratio, has been

compared with exposure of the quicklime under the moisture of air, a procedure called passive slaking, and undertaken at two different relative humidities, 60 and  $80 \pm 5$  %. Although unconventional and less common, the last two slaking methods have sometimes been reported in literature, as air-slaking. At the same time, the way in which passive slaking have been carried out here can be compared to the storage of NHL quicklime that is carried out in some industry, when only one kiln is available, and the three types of NHL need to be produced continuously. In this context, it has been considered crucial to understand the evolution of the mineralogy, microstructure and final mortar properties of the NHL when it is slaked under different methods.

The results indicate that the slaking method (conventional or passive) influences both the amount of portlandite that forms due to hydration of the calcium oxide, and the crystalline structure it develops. Thus, CaO hydration is more homogeneous and faster under conventional slaking, and a higher content of crystalline/ordered portlandite is generally formed. Under passive slaking, complete hydration of calcium oxide is ensured, especially at 80 % RH, but at a slower rate (from 15 to 30 days), and the portlandite develops mostly a disordered structure.

This study has also demonstrated that pre-hydration of hydraulic phases, such as dicalcium silicate ( $C_2S$ ) and calcium aluminates ( $C_3A$  and  $C_4AF$ ), cannot be totally prevented during both conventional and passive slaking, even though this pre-hydration is slightly reduced when quicklimes are exposed at 60 % RH. This seems to have a certain impact on the mechanical properties of the mortars, which are slightly improved when the lime is passively slaked under this relative humidity. This has been related with a higher availability of  $C_2S$  towards hydration, and therefore with a higher early-development of C-S-H in the mortar, as well as to a better adhesion between the matrix and the aggregates.

In summary, this study shows that, if the quicklime needs to be stored right after calcination, keeping it for minimum 2 weeks in an aired environment with  $RH \geq 60$  %, and providing periodically mixing, would guarantee passive slaking during storage, without the need of further water addition before it use. This process would imply both an environmental and economic benefit, as less amount of water would be consumed in the industrial manufacturing of natural hydraulic limes.

#### Authors statement

All the authors are aware of the submission of this revised version.

#### CRediT authorship contribution statement

**Clara Parra-Fernández:** Writing – original draft, Software, Methodology, Investigation, Formal analysis, Data curation. **Anna Arizzi:** Writing – review & editing, Visualization, Validation, Supervision, Project administration, Investigation, Funding acquisition, Data

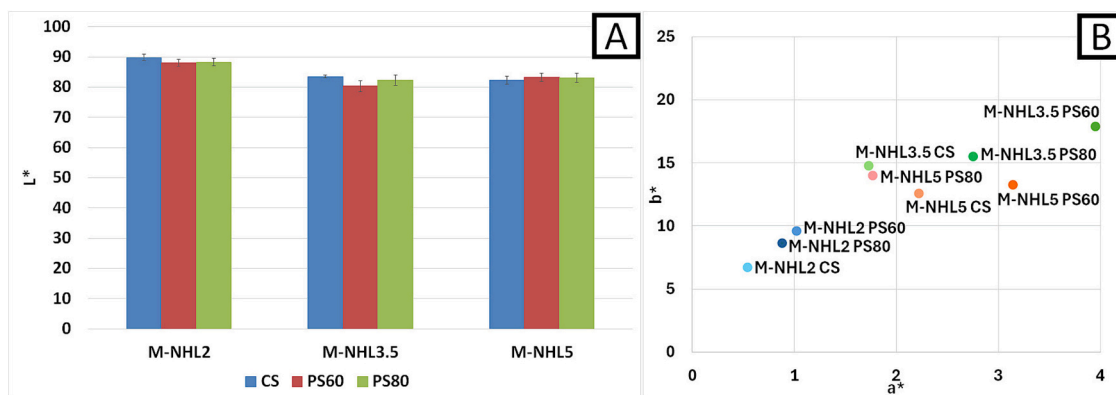


Fig. 8. Graphical representation of A: the lightness values ( $L^*$ ) and B: the colour parameters  $b^*$  versus  $a^*$  of the mortars. CS: conventional slaking; PS60: passive slaking at  $60 \pm 5$  % RH; PS80: passive slaking at  $80 \pm 5$  % RH.

curation, Conceptualization.

### Declaration of competing interest

- the work described has not been published previously.
- the article is not under consideration for publication elsewhere.
- the article's publication is approved by all authors and tacitly or explicitly by the responsible authorities where the work was carried out.
- if accepted, the article will not be published elsewhere in the same form, in English or in any other language, including electronically, without the written consent of the copyright-holder.

All authors should have made substantial contributions to all of the following:

1. The conception and design of the study.
2. Drafting the article and revising it critically for important intellectual content.
3. Final approval of the version to be submitted.

### Acknowledgements

This research is funded by the State Research Agency (SRA) and the Spanish Ministry of Innovation and Science, as part of the projects PID2020-119838RA-I00 (2021-2024) and PID2023-146405OB-I00 (2024-2027, funded by MICIU/AEI/10.13039/501100011033 and FEDER, UE), and by the Research Group RNM179 of the Junta de Andalucía. We thank Prof. Michele Secco of the University of Padova (Italy), for the valuable discussion on the structural disorder of portlandite. We are also grateful to TESELA SL (Materials, Innovation and Heritage, Spain) for providing access to their mechanical press. Funding for open access publishing: Universidad de Granada/CBUA.

### Data availability

Data will be made available on request.

### References

- [1] Boynton, R. S. Chemistry and technology of lime and limestone. second ed.. John Wiley and Sons, Inc., New York, 1980.
- [2] K.W. Ray, F.C. Mathers, Effect of temperature and time of burning upon the properties of high-calcium lime, *Ind. Eng. Chem. Res.* 20 (1928) 415–419, <https://doi.org/10.1021/ie50220a030>.
- [3] A. Moropoulou, A. Bakolas, E. Aggelakopoulou, The effects of limestone characteristics and calcination temperature to the reactivity of the quicklime, *Cem. Concr. Res.* 31 (2001) 633–639, [https://doi.org/10.1016/S0008-8846\(00\)00490-7](https://doi.org/10.1016/S0008-8846(00)00490-7).
- [4] M. Lezzerini, L. Cinzi, S. Pagnotta, Lime reactivity and overburning: the case of limestones belonging to Tuscan nappes sequence (NW Tuscany, Italy), *J. Therm. Anal. Calorim.* 149 (2024) 10577–10586, <https://doi.org/10.1007/s10973-024-13484-y>.
- [5] J. Válek, E. Van Halem, A. Viani, M. Pérez-Estébanez, R. Ševčík, P. Šašek, Determination of optimal burning temperature ranges for production of natural hydraulic limes, *Construct. Build Mater.* 66 (2014) 771–780, <https://doi.org/10.1016/j.conbuildmat.2014.06.015>.
- [6] C. Parra-Fernández, A. Arizzi, M. Secco, G. Cultrone, The manufacture of natural hydraulic limes: influence of raw materials' composition, calcination and slaking in the crystal-chemical properties of binders, *Cem. Concr. Res.* 185 (2024) 107631, <https://doi.org/10.1016/j.cemconres.2024.107631>.
- [7] S.K. Afridi, M.B. Bhatti, A.S. Ahmed, M.T. Saeed, S. Ahmad, Experimental study of calcination-carbonation process for the production of precipitated calcium carbonate, *J. Chem. Soc. Pak.* 30 (2008) 559–562.
- [8] D. Carran, J. Hughes, A. Leslie, C. Kennedy, The effect of calcination time upon the slaking properties of quicklime. J. Válek, J. Hughes, C. J. W. P. Groot (Eds.), *Historic mortars: characterisation, assessment and repair*, RILEM Bookseries, vol 7, Springer, Dordrecht, Netherlands (2012) 283–295. [https://doi.org/10.1007/978-94-007-4635-0\\_22](https://doi.org/10.1007/978-94-007-4635-0_22).
- [9] M. Zhu, J. Wu, Z. Yang, Y. Zhu, Q. Rong, Q. Wen, Effect of the textures and particle sizes of limestone on the quicklime reaction activity, *Minerals* 13 (2023) 1201, <https://doi.org/10.3390/min13091201>.
- [10] G. Vola, P. Bresciani, E. Rodeghero, L. Sarandrea, G. Cruciani, Impact of rock fabric, thermal behavior, and carbonate decomposition kinetics on quicklime industrial production and slaking reactivity, *J. Therm. Anal. Calorim.* 136 (2019) 967–993, <https://doi.org/10.1007/s10973-018-7769-7>.
- [11] G. Vola, L. Sarandrea, M. Mazzieri, P. Bresciani, M. Ardit, G. Cruciani, Reactivity and overburning tendency of quicklime burnt at high temperature, *ZKG Int.* 72 (2019) 20–31.
- [12] P. Kozlovcev, J. Válek, The micro-structural character of limestone and its influence on the formation of phases in calcined products: natural hydraulic limes and cements, *Mater. Struct./Mater. Constr.* 54 (2021) 1–27, <https://doi.org/10.1617/s11527-021-01814-7>.
- [13] G. Vola, M. Ardit, G. Frijia, F. Di Benedetto, F. Fornasier, F. Lugli, C. Natali, L. Sarandrea, K.E. Schmitt, A. Cipriani, Characterization and provenance of carbonate rocks for quicklime and Dolomite production in twin-shaft regenerative kilns from the Arabian peninsula and neighboring countries, *Minerals* 13 (2023) 1500, <https://doi.org/10.3390/min13121500>.
- [14] G. Leontakianakos, I. Baziotis, A. Papandreou, D. Kanellopoulou, V. N. Stathopoulos, S. Tsimas, A comparative study of the physicochemical properties of mg-rich and ca-rich quicklimes and their effect on reactivity, *Mater. Struct./Mater. Constr.* 48 (2015) 3735–3753, <https://doi.org/10.1617/s11527-014-0436-y>.
- [15] J.M. Commandré, S. Salvador, A. Nzihou, Reactivity of laboratory and industrial limes, *Chem. Eng. Res. Des.* 85 (2007) 473–480, <https://doi.org/10.1205/cherd06200>.
- [16] Artioli, G., Secco, M., Addis, A. The Vitruvian legacy: Mortars and binders before and after the Roman world. Artioli, G., Oberti, R. (Eds.). *The contribution of mineralogy to cultural heritage*, EMU Notes, 20 (2019) 151–202. <https://doi.org/10.1180/EMU-notes.20.4>.
- [17] K. Elert, C. Rodríguez-Navarro, E. Sebastián-Pardo, E. Hansen, O. Cazalla, Lime mortars for the conservation of historic buildings, *Stud. Conserv.* 47 (2002) 62–75, <https://doi.org/10.1179/sic.2002.47.1.62>.
- [18] CEN, European Committee for Standardization (Ed.), EN 459–2. *Building lime - part 2: test methods*, 2021.
- [19] ASTM C25., Standard test methods for chemical analysis of limestone, quicklime, and hydrated lime, *ASTM Book Stand.* 04 (01) (2017) 28–30.
- [20] J.H. Potgieter, S.S. Potgieter, B. Legodi, Proposed modifications to the method for the determination of available lime, *Miner. Eng.* 14 (2001) 515–523, [https://doi.org/10.1016/S0892-6875\(01\)00039-5](https://doi.org/10.1016/S0892-6875(01)00039-5).
- [21] J.A.H. Oates, *Lime and limestone: chemistry and technology, production and uses*, Wiley-VCH, Weinheim, Germany, 1998.
- [22] J.H. Potgieter, S.S. Potgieter, S.J. Moja, A. Mulaba-Bafubandi, An empirical study of factors influencing lime slaking. Part I: production and storage conditions, *Miner. Eng.* 15 (2002) 201–203, [https://doi.org/10.1016/S0892-6875\(02\)00008-0](https://doi.org/10.1016/S0892-6875(02)00008-0).
- [23] K. Balksten, B.M. Steenari, The influence of particle size and structure in hydrated lime on the properties of the lime putty and lime mortar, *Int. J. Archit. Herit.* 4 (2010) 86–101, <https://doi.org/10.1080/15583050902822681>.
- [24] S.A. Hassan, A.A. Al-Zahrani, Slaking lime for restoration and conservation of historical buildings and materials, criticism of an Arabic historical manuscript, *Eng. Appl. Sci.* 2 (2017) 125–131, <https://doi.org/10.11648/j.eas.20170206.15>.
- [25] S. Dai, Preliminary study on wind slaked lime used before Qing dynasty in China, *J. Archit. Conserv.* 24 (2018) 91–104, <https://doi.org/10.1080/13556207.2018.1491136>.
- [26] B. Tomazic, R. Mohanty, M. Tadros, J. Estrin, Crystallization of calcium hydroxide from aqueous solution. A preliminary study, *J. Cryst. Growth* 75 (1986) 329–338, [https://doi.org/10.1016/0022-0248\(86\)90047-3](https://doi.org/10.1016/0022-0248(86)90047-3).
- [27] C. Rodríguez-Navarro, E. Hansen, W.S. Ginell, Calcium hydroxide crystal evolution upon aging of lime putty, *J. Am. Ceram. Soc.* 81 (1998) 3032–3034, <https://doi.org/10.1111/j.1151-2916.1998.tb02735.x>.
- [28] O. Cazalla, C. Rodríguez-Navarro, E. Sebastian, G. Cultrone, M.J. De la Torre, Aging of lime putty: effects on traditional lime mortar carbonation, *J. Am. Ceram. Soc.* 83 (2000) 1070–1076, <https://doi.org/10.1111/j.1151-2916.2000.tb01332.x>.
- [29] E.F. Hansen, A. Tagle, E. Erder, S. Baron, S. Connell, C. Rodriguez-Navarro, K. Van Balen, Effects of ageing on lime putty, in: *International RILEM Workshop on Historic Mortars: Characteristics and Tests*, RILEM Publications sarl, Cachan, France, 2000, pp. 197–206.
- [30] M.G. Margalha, M.R. Veiga, J. de Brito, The maturation time factor on the lime putty quality, in: *In: 7th International Brick Masonry Conference*, London, UK, 2006.
- [31] W. Gallala, M.E. Gaied, A. Tlili, M. Montacer, Factors influencing the reactivity of quicklime, *Proc. Inst. Civ. Eng.: Constr. Mater.* 161 (2008) 25–30, <https://doi.org/10.1680/coma.2008.161.1.25>.
- [32] G.F. Wei, B.J. Zhang, S.Q. Fang, Aging mechanism of quicklime and application study of aged lime in conservation of cultural relics, *J. Build. Mater.* 15 (2012) 96–102.
- [33] M.C. Mascolo, V. Daniele, G. Mascolo, An approach for a rapid determination of the aging time of lime putty, *Thermochim. Acta* 648 (2017) 75–78, <https://doi.org/10.1016/j.tca.2016.12.012>.
- [34] A. El-Turki, R.J. Ball, G.C. Allen, The influence of relative humidity on structural and chemical changes during carbonation of hydraulic lime, *Cem. Concr. Res.* 37 (2007) 1233–1240, <https://doi.org/10.1016/j.cemconres.2007.05.002>.
- [35] Ö. Cizer, K. Van Balen, D.A. Van Gemert, Competition between hydration and carbonation in hydraulic lime and lime-pozzolana mortars, *Adv. Mater. Res.* 133-134 (2010) 241–246, <https://doi.org/10.4028/www.scientific.net/AMR.133-134.241>.

- [36] S. Xu, J. Wang, Y. Sun, Effect of water binder ratio on the early hydration of natural hydraulic lime, *Mater. Struct./Mater. Constr.* 48 (2015) 3431–3441, <https://doi.org/10.1617/s11527-014-0410-8>.
- [37] J. Lanás, J.L. Pérez Bernal, M.A. Bello, J.I. Álvarez Galindo, Mechanical properties of natural hydraulic lime-based mortars, *Cem. Concr. Res.* 34 (2004) 2191–2201, <https://doi.org/10.1016/j.cemconres.2004.02.005>.
- [38] D. Zhang, J. Zhao, D. Wang, C. Xu, M. Zhai, X. Ma, Comparative study on the properties of three hydraulic lime mortar systems: natural hydraulic lime mortar, cement-aerial lime-based mortar and slag-aerial lime-based mortar, *Construct. Build Mater.* 186 (2018) 42–52, <https://doi.org/10.1016/j.conbuildmat.2018.07.053>.
- [39] L. Fusade, H.A. Viles, A comparison of standard and realistic curing conditions of natural hydraulic lime repointing mortar for damp masonry: impact on laboratory evaluation, *J. Cult. Herit.* 37 (2019) 82–93, <https://doi.org/10.1016/j.culher.2018.11.011>.
- [40] C. Groot, R. Veiga, I. Papayianni, R. Van Hees, M. Secco, J.I. Álvarez, P. Faria, M. Stefanidou, RILEM TC 277-LHS report: lime-based mortars for restoration—a review on long-term durability aspects and experience from practice, *Mater. Struct./Mater. Constr.* 55 (2022) 245, <https://doi.org/10.1617/s11527-022-02052-1>.
- [41] P. Kozlovcev, G. Triantafyllou, R. Prikryl, A. Soultana, J. Prikrylova, Mechanical Properties of Mortar Specimens Prepared from Experimentally Burnt Impure Limestones: Effect of Raw Material Characteristics and Burning Conditions, *EGU Gen. Assem. Conf. Abstr.* 2017, p. 18684.
- [42] M. Lezzerini, S. Legnaioli, S. Pagnotta, V. Palleschi, The source materials for lime production in the Monte Pisano area (NW Tuscany, Italy), *IOP Conf. Ser.: Earth Environ. Sci.* 609 (2020) 012078, <https://doi.org/10.1088/1755-1315/609/1/012078>.
- [43] E.C. Eckel, *Cement, limes and plasters: their materials, manufacture and properties*, John Wiley and Sons, London, 1922.
- [44] A.D. Cowper, *Lime and lime mortars 14*, Donhead Publishing Ltd, Shaftesbury, 1927.
- [45] S. Holmes, M. Wingate, *Building with lime: a practical introduction 12-14*, Intermediate Technology Publications Ltd, Warwickshire, 1997.
- [46] P.F.G. Banfill, A.M. Foster, A relationship between hydraulicity and permeability of hydraulic lime. In: P. Bartos, C. Groot, J.J. Hughes (eds.), *international RILEM workshop on historic mortars: characteristics and tests*, RILEM publications sarl, Cachan, pp. 173–183, 2000.
- [47] H. Böke, Ö. Çizer, B. İpekoğlu, E. Uğurlu, K. Şerifaki, G. Toprak, Characteristics of lime produced from limestone containing diatoms, *Construct. Build Mater.* 22 (2008) 866–874, <https://doi.org/10.1016/j.conbuildmat.2006.12.010>.
- [48] Elsen, J., Mertens, G., Snellings, R. Portland cement and other calcareous hydraulic binders: History, production and mineralogy. Christidis, G.E., *Advances in the characterization of industrial minerals*. European Mineralogical Union Notes in Mineralogy, 9. London: London, 2010, pp. 441–479. <https://doi.org/10.1180/EMU-notes.9.11>.
- [49] J.Elsen, VanK.Balen, G.Mertens. Hydraulicity in historic lime mortars: A review, in: J.Válek, J.J.Hughes, C.J.W.P.Groot (Eds.), *Historic mortars*, RILEM Bookseries, Springer Netherlands, 2012, pp. 125–139. [https://doi.org/10.1007/978-94-007-4635-0\\_10](https://doi.org/10.1007/978-94-007-4635-0_10).
- [50] P. Kozlovcev, R. Prikryl, Devonian micritic limestones used in the historic production of Prague hydraulic lime ('pasta di Praga'): characterization of the raw material and experimental laboratory burning, *Mater. Constr.* 65 (2015) 1–16, <https://doi.org/10.3989/mc.2015.06314>.
- [51] H.M. Rietveld, A profile refinement method for nuclear and magnetic structures, *J. Appl. Cryst.* 2 (1969) 65–71, <https://doi.org/10.1107/S0021889869006558>.
- [52] EN 196-1. *Methods of Testing Cement. Determination of Strength*, CEN, European Committee for Standardization, 2016.
- [53] EN 1015-6., *Methods of Test for Mortar for Masonry - Part 6: Determination of Bulk Density of Fresh Mortar*, CEN, European Committee for Standardization, 1998.
- [54] EN 1015-3., *Methods of Test for Mortar for Masonry. Determination of Consistence of Fresh Mortar (by Flow Table)*, CEN, European Committee for Standardization, 1999.
- [55] CEN, European Committee for Standardization (Ed.), EN 1015-11. *Methods of test for mortar for masonry - part 11: determination of flexural and compressive strength of hardened mortar*, 2019.
- [56] CEN, European Committee for Standardization (Ed.), EN 12407, *natural stone test methods - petrographic examination*, 2019.
- [57] CEN, European Committee for Standardization (Ed.), EN 459-1, *Building lime - part 1: definitions, specifications and conformity criteria*, 2015.
- [58] M. Atasever, S.T. Erdoğan, Effects of clay type and component fineness on the hydration and properties of limestone calcined clay cement, *Mater. Struct.* 57 (2024) 183, <https://doi.org/10.1617/s11527-024-02461-4>.
- [59] M.R.C. Da Silva, J.D.S. Andrade Neto, B. Walkley, A.P. Kirchheim, Effects of kaolinite and montmorillonite calcined clays on the sulfate balance, early hydration, and artificial pore solution of limestone calcined clay cements (LC3), *Mater. Struct.* 57 (2024) 187, <https://doi.org/10.1617/s11527-024-02462-3>.
- [60] P. Kozlovcev, R. Prikryl, Compositional characteristics and experimental burning of selected lower Palaeozoic limestones from the Prague Basin (Barrandian area, Czech Republic) suitable for the production of natural hydraulic lime, *Bull. Eng. Geol. Environ.* 76 (2017) 21–37, <https://doi.org/10.1007/s10064-016-0882-6>.
- [61] J.E. Gillott, Carbonation of  $\text{Ca}(\text{OH})_2$  investigated by thermal and X-ray diffraction methods of analysis, *J. Appl. Chem.* 17 (1967) 185–189, <https://doi.org/10.1002/jctb.5010170701>.
- [62] O. Chaix-Pluchery, J. Pannetier, J. Bouillot, J.C. Niepce, Structural pre-reactional transformations in  $\text{Ca}(\text{OH})_2$ , *J. Solid State Chem.* 67 (1987) 225–234, [https://doi.org/10.1016/0022-4596\(87\)90358-6](https://doi.org/10.1016/0022-4596(87)90358-6).
- [63] A.F. Gualtieri, A. Viani, C. Montanari, Quantitative phase analysis of hydraulic limes using the Rietveld method, *Cem. Concr. Res.* 36 (2006) 401–406, <https://doi.org/10.1016/j.cemconres.2005.02.001>.
- [64] M. Lassinantti Gualtieri, M. Romagnoli, P. Miselli, M. Cannio, A.F. Gualtieri, Full quantitative phase analysis of hydrated lime using the Rietveld method, *Cem. Concr. Res.* 42 (2012) 1273–1279, <https://doi.org/10.1016/j.cemconres.2012.05.016>.
- [65] K. Kudlacz, C. Rodriguez-Navarro, The mechanism of vapor phase hydration of calcium oxide: implications for  $\text{CO}_2$  capture, *Environ. Sci. Technol.* 48 (2014) 12411–12418, <https://doi.org/10.1021/es5034662>.
- [66] C. Rodriguez-Navarro, A. Burgos-Cara, F.D. Lorenzo, E. Ruiz-Agudo, K. Elert, Nonclassical crystallization of calcium hydroxide via amorphous precursors and the role of additives, *Cryst. Growth Des.* 20 (2020) 4418–4432, <https://doi.org/10.1021/acs.cgd.0c00241>.
- [67] H.G. Midgley, The determination of calcium hydroxide in set Portland cements, *Cem. Concr. Res.* 9 (1979) 77–82, <https://doi.org/10.1016/0008-8846%2879%2990097-8>.
- [68] N.B. Milestone, Hydration of tricalcium silicate in the presence of lignosulfonates, glucose, and sodium gluconate, *J. Am. Ceram. Soc.* 62 (1979) 321–324, <https://doi.org/10.1111/j.1151-2916.1979.tb19068.x>.
- [69] A.G. De la Torre, A. Cabeza, A. Calvente, S. Bruque, M.A. Aranda, Full phase analysis of Portland clinker by penetrating synchrotron powder diffraction, *Anal. Chem.* 73 (2001) 151–156, <https://doi.org/10.1021/ac0006674>.
- [70] N.V.Y. Scarlett, I.C. Madsen, C. Manias, D. Retalack, On-line X-ray diffraction for quantitative phase analysis: application in the Portland cement industry, *Powder Diffract.* 16 (2001) 71–80, <https://doi.org/10.1154/1.1359796>.
- [71] G. Vola, *High-grade burnt lime products: impact of calcination kinetics on slaking reactivity; sticking tendency and blocks formation at HT (1300° C)*. PhD thesis, Università degli Studi di Ferrara., 2019.
- [72] G. Leontakianakos, I. Baziotis, V.N. Stathopoulos, Z. Kyritidou, L. Profitis, E. Chatzitheodoridis, S. Tsimas, Influence of natural water composition on reactivity of quicklime derived from Ca-rich and Mg-rich limestone: implications for sustainability of lime manufacturing through geochemical modeling, *RSC Adv.* 6 (2016) 65799–65807, <https://doi.org/10.1039/C6RA11346J>.
- [73] Ç. Hoşten, M. Gülsün, Reactivity of limestones from different sources in Turkey, *Miner. Eng.* 17 (2004) 97–99, <https://doi.org/10.1016/j.mineng.2003.10.009>.
- [74] P. Agrinier, A. Deutsch, U. Schärer, I. Martínez, Fast back-reactions of shock-released  $\text{CO}_2$  from carbonates: an experimental approach, *Geochim. Cosmochim. Acta* 65 (2001) 2615–2632, [https://doi.org/10.1016/S0016-7037\(01\)00617-2](https://doi.org/10.1016/S0016-7037(01)00617-2).
- [75] W.G. Mumme, R.J. Hill, G. Bushnell-Wye, E.R. Segnit, *Neues Mineral.* 169 (1995) 35–68.
- [76] M. Stankeviciute, R. Siauciunas, A. Miachai, Impact of  $\alpha$ -C<sub>2</sub>S<sub>H</sub> calcination temperature on the mineral composition and heat flow of the products, *J. Therm. Anal. Calorim.* 134 (2018) 101–110, <https://doi.org/10.1007/s10973-018-7548-5>.
- [77] F. Nishi, Y. Takeuchi, I. Maki, Tricalcium silicate  $\text{Ca}_3\text{O}[\text{SiO}_4]$ : the monoclinic superstructure, *Z. fur Krist. - Cryst. Mater.* 172 (1–4) (1985) 297–314, <https://doi.org/10.1524/zkri.1985.172.14.297>.
- [78] K. Callebaut, J. Elsen, K. Van Balen, W. Viaene, Nineteenth century hydraulic restoration mortars in the Saint Michael's church (Leuven, Belgium): natural hydraulic lime or cement? *Cem. Concr. Res.* 31 (2001) 397–403, [https://doi.org/10.1016/S0008-8846\(00\)00499-3](https://doi.org/10.1016/S0008-8846(00)00499-3).
- [79] P. Mondal, J.W. Jeffery, The crystal structure of tricalcium aluminate,  $\text{Ca}_3\text{Al}_2\text{O}_6$ , *Acta Crystallogr. B Struct. Sci. Cryst. Eng. Mater.* 31 (3) (1975) 689–697, <https://doi.org/10.1107/S0567740875003639>.
- [80] A.A. Colville, S. Geller, The crystal structure of brownmillerite,  $\text{Ca}_2\text{FeAlO}_6$ , *Acta Crystallogr. B Struct. Sci. Cryst. Eng. Mater.* 27 (12) (1971) 2311–2315, <https://doi.org/10.1107/S056774087100579X>.
- [81] D. Moseley, F.P. Glasser, Properties and composition of bredigite-structured phases, *J. Mater. Sci.* 17 (1982) 2736–2740, <https://doi.org/10.1007/BF00543911>.
- [82] C. Shao, Z. Xu, Z. Liu, Y. Zhang, D. Wang, Effect of hydration degrees on the accelerated carbonization (3%  $\text{CO}_2$ ) behavior of natural hydraulic lime, *Construct. Build Mater.* 438 (2024) 137297, <https://doi.org/10.1016/j.conbuildmat.2024.137297>.
- [83] B. Kostura, H. Kulveitová, J. Leško, Blast furnace slags as sorbents of phosphate from water solutions, *Water Res.* 39 (9) (2005) 1795–1802, <https://doi.org/10.1016/j.watres.2005.03.010>.
- [84] P.A. Sabine, M.T. Styles, B.R. Young, The nature and paragenesis of natural bredigite and associated minerals from Carneal and Scawt Hill, Co. Antrim, *Mineral. Mag.* 49 (354) (1985) 663–670, <https://doi.org/10.1180/minmag.1985.049.354.05>.
- [85] T. Sopcak, L. Medvecký, P. Jevinova, M. Giretova, A. Mahun, L. Kobera, R. Stulajterova, F. Kromka, V. Girman, M. Balaz, Physico-chemical, mechanical and antibacterial properties of the boron modified biphasic larnite/bredigite cements for potential use in dentistry, *Ceram. Int.* 49 (4) (2023) 6531–6544, <https://doi.org/10.1016/j.ceramint.2022.10.119>.
- [86] F. Winnefeld, L.H. Martin, C.J. Müller, B. Lothenbach, Using gypsum to control hydration kinetics of CSA cements, *Construct. Build Mater.* 155 (2017) 154–163, <https://doi.org/10.1016/j.conbuildmat.2017.07.217>.
- [87] M. Palou, J. Majling, M. Dová, J. Kozanková, S.C. Mojmudar, Formation and stability of crystallohydrates in the non-equilibrium system during hydration of SAB cements, *Ceram. - Silik.* 49 (4) (2005) 230–236.

- [88] F. Tavangarian, R. Emadi, Mechanism of nanostructure bredigite formation by mechanical activation with thermal treatment, *Mater. Lett.* 65 (15–16) (2011) 2354–2356, <https://doi.org/10.1016/j.matlet.2011.04.108>.
- [89] S.M. Mirhadi, F. Tavangarian, R. Emadi, Synthesis, characterization and formation mechanism of single-phase nanostructure bredigite powder, *Mater. Sci. Eng. C* 32 (2) (2012) 133–139, <https://doi.org/10.1016/j.msec.2011.10.007>.
- [90] E. Dubina, L. Korat, L. Black, J. Strupi-Šuput, J. Plank, Influence of water vapour and carbon dioxide on free lime during storage at 80 °C, studied by raman spectroscopy, *Spectrochim. Acta - A: Mol. Biomol. Spectrosc.* 111 (2013) 299–303, <https://doi.org/10.1016/j.saa.2013.04.033>.
- [91] S.S. Potgieter, C.A. Strydom, O. Gheevarhese, The effect of ultrasonic energy on lime slaking, *Miner. Eng.* 16 (2003) 767–770, [https://doi.org/10.1016/S0892-6875\(03\)00173-0](https://doi.org/10.1016/S0892-6875(03)00173-0).
- [92] L.N. Warr, IMA-CNMNC approved mineral symbols, *Mineral. Mag.* 85 (2021) 291–320, <https://doi.org/10.1180/mgm.2021.43>.
- [93] J. Lanás, J. Alvarez, Dolomitic limes: evolution of the slaking process under different conditions, *Thermochim. Acta* 423 (2004) 1–12, <https://doi.org/10.1016/j.tca.2004.04.016>.
- [94] B.Z. Dilnesa, B. Lothenbach, G. Renaudin, A. Wichser, D. Kulik, Synthesis and characterization of hydrogarnet  $\text{Ca}_3(\text{Al}_x\text{Fe}_{1-x})_2(\text{SiO}_4)_y(\text{OH})_{4(3-y)}$ , *Cem. Concr. Res.* 59 (2014) 96–111, <https://doi.org/10.1016/j.cemconres.2014.02.001>.
- [95] T. Matschei, B. Lothenbach, F.P. Glasser, The role of calcium carbonate in cement hydration, *Cem. Concr. Res.* 37 (2007) 551–558, <https://doi.org/10.1016/j.cemconres.2006.10.013>.
- [96] A. Arizzi, G. Cultrone, Mortars and plasters—how to characterise hydraulic mortars, *Archaeol. Anthropol. Sci.* 13 (2021) 144, <https://doi.org/10.1007/s12520-021-01404-2>.
- [97] D. Damidot, S. Stronach, A. Kindness, M. Atkins, F.P. Glasser, Thermodynamic investigation of the  $\text{CaO-Al}_2\text{O}_3\text{-CaCO}_3\text{-H}_2\text{O}$  closed system at 25 °C and the influence of  $\text{Na}_2\text{O}$ , *Cem. Concr. Res.* 24 (1994) 563–572, <https://doi.org/10.1680/acr.1995.7.27.129>.
- [98] A. Ipavec, R. Gabrovšek, T. Vuk, V. Kaučič, J. Maček, A. Meden, Carboaluminate phases formation during the hydration of calcite-containing Portland cement, *J. Am. Ceram. Soc.* 94 (2011) 1238–1242, <https://doi.org/10.1111/j.1551-2916.2010.04201.x>.
- [99] A. Mesbah, J.P. Rapin, M. François, C. Cau-dit-Coumes, F. Frizon, F. Leroux, G. Renaudin, Crystal structures and phase transition of cementitious bi-anionic AFm-( $\text{Cl}^-$ ,  $\text{CO}_3^{2-}$ ) compounds, *J. Am. Ceram. Soc.* 94 (2011) 261–268, <https://doi.org/10.1111/j.1551-2916.2010.04050.x>.
- [100] L.G. Baquerizo, T. Matschei, K.L. Scrivener, M. Saeidpour, L. Wadsö, Hydration states of AFm cement phases, *Cem. Concr. Res.* 73 (2015) 143–157, <https://doi.org/10.1016/j.cemconres.2015.02.011>.
- [101] Taylor, H.F.W. *Cement chemistry*, second ed.. Thomas Telford Publishing, London, 1997.
- [102] A. Henry, J. Stewart, *English Heritage, Practical building conservation. Mortars, renders & plasters*, Ashgate, Farnham, 2012.
- [103] C. Figueiredo, M. Lawrence, R.J. Ball, Chemical and physical characterization of three NHL2 and the relationship with the mortar properties, in: L. Villegas, I. Lombillo, H. Blanco, Y. Boffill (Eds.), REHABEND euro-american congress: construction pathology, rehabilitation technology and heritage management (6th REHABEND Congress), Burgos, CODE: vol. 2.2.17, pp. 1–8., 2016.
- [104] Figueiredo C, Henry A, Holmes S, Hydraulic lime production coming full circle? Cathedral Communications. Celebrating twenty-five years of the Building Conservation Directory 1993–2018; pp. 134–142. <https://www.buildingconservation.com/books/bcd2018/134/>, 2018 (accessed 20 May 2024).
- [105] C. Figueiredo, Properties and performance of lime mortars for conservation: the role of binder chemistry and curing regime. PhD thesis, university of bath., 2018.
- [106] S.J. Oh, Comparative Laboratory Evaluation of Natural Hydraulic Lime Mortars for Conservation, PhD Thesis, Columbia University, 2020, <https://doi.org/10.7916/d8-yrrn-9w25>.
- [107] J.I. Álvarez, R. Viega, S. Martínez-Ramírez, M. Secco, P. Faria, P.N. Maravelaki, M. Ramesh, I. Papayanni, J. Válek, RILEM TC 277-LHS, Report: a review on the mechanisms of setting and hardening of lime-based binding systems, *Mater. Struct.* 54 (2021) 63–1–30, <https://doi.org/10.1617/s11527-021-01648-3>.
- [108] Lea, F. M. *The chemistry of cement and concrete*, third ed.. Chemical Publishing, New York, 1970.
- [109] A. Bahhou, Y. Taha, R. Hakkou, M. Benzaazoua, A. Tagnit-Hamou, Assessment of hydration, strength, and microstructure of three different grades of calcined marls derived from phosphate by-products, *J. Build. Eng.* 84 (2024) 108640, <https://doi.org/10.1016/j.jobte.2024.108640>.
- [110] C. Parra-Fernández, M. Varas-Muriel, Petrographic and petrophysical characterization of the main aerial and hydraulic mortars used in the construction and rehabilitation sectors, *Mater. Constr.* 75 (2025) e367, <https://doi.org/10.3989/mc.2025.379124>.
- [111] C. Pesce, M.C. Godina, A. Henry, G. Pesce, Towards a better understanding of hot-mixed mortars for the conservation of historic buildings: the role of water temperature and steam during lime slaking, *Herit. Sci.* 9 (2021) 72, <https://doi.org/10.1186/s40494-021-00546-9>.